ON THE PREDICTED AND OBSERVED COLOR BOUNDARIES OF THE RR LYRAE INSTABILITY STRIP AS A FUNCTION OF METALLICITY

ALLAN SANDAGE

The Observatories of the Carnegie Institution of Washington, 813 Santa Barbara Street, Pasadena California, 91101

ABSTRACT

The purpose of the paper is to predict the temperature at the fundamental blue edge (FBE) of the instability strip for RR Lyrae (RRL) variables from the pulsation equation that relates temperature to period, luminosity, and mass. Modern data for the correlations between period, luminosity, and metallicity at the FBE for field and cluster RRL are used for the temperature calculation. The predicted temperatures are changed to B-V colors using an adopted color transformation. The predicted temperatures at the FBE become hotter as [Fe/H] changes from 0 to -1.5, and thereafter cooler as the metallicity decreases to -2.5 and beyond. The temperature range over this interval of metallicity is Δlog T_e = 0.04, or 640 K at 6900K. The predicted color variation is at the level of 0.03 mag in B-V. The predictions are compared with the observed RRL colors at the FBE for both the field and cluster variables, showing general agreement at the level of 0.02 mag in $(B-V)_o$, which, however, is the uncertainty of the reddening corrections.

The focus of the problem is then reversed by fitting a better envelope to the observed FBE relation between color and metallicity for metallicities smaller than -1.8 which, when inserted in the pulsation equation, gives a non-linear calibration of the absolute magnitude of the average evolved level of the HB of M_V = 1.109 + 0.600 ([Fe/H]) + 0.140 $([Fe/H])^2$, where the zero point has been set by the observed RR Lyrae stars in the LMC at $\langle V \rangle_o$ = 19.064 for [Fe/H] = -1.5, and using an adopted LMC modulus of $(m-M)_o$ = 18.54.

The position of the envelope locus at the shortest periods for the observed period-metallicity correlation differs between the field and cluster variables by Δlog P = 0.029 $\pm$ 0.007, the field variables having the shorter periods at the envelope. The field and cluster variables also differ in the near absence of cluster RR Lyraes in the -1.7 > [Fe/H] > -2.0 metallicity interval, whereas the field

variables show no such gap. We aver that these differences require different origins for the field and the cluster variables.

A test is proposed by comparing the morphology of the horizontal branches in the local dwarf spheroidals with that in the Galactic globular clusters in the inner halo and by relating the differences with the relevant second parameter indicators.

Subject headings: stars: RR Lyrae–stars: luminosities–stars: horizontal branch–clusters: globular–galaxies: dwarf spheroidals

1. Introduction

A model was proposed at the Vatican Conference on Stellar Populations (O'Connell 1958) to explain the period-ratio dichotomy in globular cluster RR Lyrae variables, studied by Oosterhoff (1939, 1944), following its discovery by Grosse (1932) and Hachenberg (1939). The postulate of the model was that the difference in the observed mean periods between the two Oosterhoff groups could be understood if the absolute magnitude levels of the groups differed by ∼0.2 mag at constant temperature, the variables in the long period group being brighter (Sandage 1958). In the discussion, Martin Schwarzschild (1958) asked if, instead, the period ratio could be explained by a temperature difference with the long period group (Oost II) being cooler on average than Oosterhoff I clusters, keeping the luminosities the same.

I replied that a color shift would have to be at the level of 0.09 mag in B-V toward the red in the long period Oosterhoff group. Although a later calculation (Sandage 1993b, hereafter S93b, footnote 1) gave 0.06 mag for the required color shift, both 0.06 and 0.09 mag were outside the bounds permitted by the observations of clusters in the two Oosterhoff period groups known at the time for M3 and M92 (Arp, Baum, and Sandage 1953, Sandage 1953) and for five other clusters (Arp 1955) over the relevant metallicity range of -1.5 > [Fe/H] > -2.2. A near zero color difference of the blue fundamental edge of the strip for such clusters at the level of ∼0.02 mag in B-V was later confirmed from more precise photoelectric data of horizontal branch stars, and better determinations of the E(B-V) (Sandage 1969).

It was this conclusion that led to the near canonical assumption in the late 1980s that one should use a constant mean temperature of log T_e ∼3.85 for the mid point of the strip in comparing the predictions from theoretical models of the zero age horizontal branch (ZAHB) with the observations (S82a, S90b). However, this assumption of constant temperature for all metallicities led to the vigorous debate in the decades of 1985 and 1995 concerning the

adequacy of the extant ZAHB models or, in fact, whether the period shifts claimed by the observers using data on amplitudes were real (Caputo 1988; Lee 1990; Lee, Demarque, & Zinn 1990, hereafter LDZ; Brocato, Castellani, & Ripepi 1994, 1996).

Nevertheless, *continuous* period shifts with metallicity, not just a *dichotomy* of mean period ratios, had been discovered by Preston (1959, his Fig. 4) for field RR Lyraes with the non-zero slope of dlogP/d([Fe/H]) $\sim$ -0.10 in the log P-metallicity relation. The continuum with this slope was later shown beyond doubt for the bright field RR Lyraes from the larger sample of Layden (1995, his Fig. 1).

Other determinations of the slope at dlogP/d([Fe/H]) = -0.12 $\pm$ 0.02 for the period-metallicity correlation had also been derived from a variety of independent data for RRL in clusters (Sandage, Katem, & Sandage 1981, hereafter SKS; S81b, Table 7, S82a,b). Some of these determinations were from amplitude- metallicity correlations, some from rise-time-metallicity correlations, and some from period-temperature correlations within the strip as a function of metallicity.

Nevertheless, debate on the validity of period shifts determined using amplitudes remain. Now the focus has shifted from questioning the validity of the ZAHB *theoretical models*, to the role of evolution off the initial non-evolved sequence (eg. LDZ 1990; Sandage 1990a; Brocato et al. 1994, 1996; Clement & Sheldon 1999a,b; Cacciari, Corwin, & Carney 2004).

The evidence for a period-amplitude-metallicity relation at various temperatures remains as it was set out in 1981 (S81a); it has been rediscovered by Carney, Storm, & Jones [1992, their Eq. (16)], and by Alcock et al. (1998; Alcock 2000).

It is useful to recall the strong debate in the 1990s concerning the observational data on period shifts. The extant ZAHB models did not predict such shifts when the predictions were made in a particular way, and the theoreticians, believing their models, questioned the interpretation of the observations on amplitudes and temperatures. The reasons were these.

The early pioneering models of the luminosity level of the ZAHB level for different metallicitites had been made by Sweigart and Gross (1976) followed by Sweigart, Renzini, & Tornambe (1987, hereafter SRT), Bencivenni et al. (1991), and Dorman (1992). A more complete list of references is in SRT. Modern updates of these pioneering papers are, among others, those of Bono et al. (1997a), VandenBerg et al. (2000), and Catelan, Pritzl & Smith (2004), each of which contain references to other recent models.

The period shifts with metallicity could be predicted from these models in the following way. The models give calculated tracks for the ZAHB in HR diagrams of Log L, log T_e for different metallicities. They also give mass as a function of [Fe/H] along the tracks. Imposing

a constant temperature line across the tracks, generally at log $T_e = 3.85$, permitted log L and mass to be read along this fixed temperature line. A pulsation equation, P(L,M,T_e,[Fe/H]) that relates period, luminosity, and mass, is then used to predict how periods along the constant temperature line should vary with metallicity.

These predictions gave a near zero slope (S93b, Fig. 6b) to a period-metallicity correlation rather than the value of dlogP/d([Fe/H]) = -0.12 derived from the observations. The effect of the increased luminosity on the period as the metallicity is decreased was nearly cancelled by the corresponding increased mass along the ZAHB in these models, shown explicitly by Simon and Clement (1993, the first and second unnumbered equations in their section 8). And even if the effect of luminosity evolution from the ZAHB was included as in Gratton, Tornambe, & Ortolani (1986), and LDZ (1990, their Table 2), these models predicted a slope of the period-metallicity relation to be only dlogP/d([Fe/H]) = -0.05, but, again, *when read at constant temperature*. This was less than half of what is observed.

The solution of reconciling the model predictions with the observations, obvious now but not at the time, was to drop the condition of reading the models at constant temperature, but rather to let the temperature be cooler for more metal poor RRL at their higher luminosities. This solution had been proposed for RRc variables by Simon and Clement (1993) in their seminal paper on the discovery of methods to obtain luminosities, chemical abundances, masses, and temperature from various Fourier components of the light curves for RRc variables. They stated, based on their theoretical expectations, that " —it is not correct to formulate a period shift at constant temperature (eg. Sandage 1990b, ApJ 350, 631)."

The same solution of cooler temperature for the Oosterhoff II variables was proposed independently using the pulsation equation for RRab variables at the fundamental blue edge (S93a,b). It was shown there that a variation of temperature at the BFE at the rate of dlogT_e/d([Fe/H]) = -0.012 would largely reconcile the prediction from the models and the observations of period-shifts, if a mild evolution is also introduced (S93b, Fig. 6a compared to 6b).

The purpose of the present paper is to return to the problem, demonstrating more directly the need for a temperature variation with metallicity at the fundamental blue edge of the instability strip. In making the argument we reverse the dependent and independent variables in a pulsation equation by making T_e the independent variable to be determined by assuming the observed dependencies of log P, log L, and log mass on metallicity, all of which are better known now than in S93a.

The organization of the paper is as follows. Section 2 shows an updated period-

metallicity correlation using the data in the catalog of 302 field RRL with measured metallicities by Layden (1994) on the scale of Zinn and West (1984). There are nearly three times the number of field stars in the Layden sample than in the catalog by Blanco (1992) that was used in S93a.

Section 3 shows a similar period-metallicity distribution as in §2 for RRL in globular clusters from the updated catalog of cluster variables by Clement (2001) that merges the data from the third catalog of Sawyer Hogg (1973) with new data complete to 2000 from the literature, adding about 30% to the data base used in S93a.

Section 4 sets out four modern calibrations of the absolute magnitude-metallicity relation for RRL by Caputo et al. (2000), Clementini et al. (2003), Catelan, Pritzl, & Smith (2004), and McNamara et al. (2004), many of which emphasize the need for a non-linear M_V([Fe/H]) luminosity-metallicity relation both for the ZAHB and for the evolved HB. These four are a representative subset of many other current calibrations, reviewed by Cacciari and Clementini (2004).

A new calibration of the mass-metallicity relation calculated by Bono et al. (1997a) is given in §5, and compared with that of Dorman (1992) that was used in S93a.

In §6 we combine the period-metallicity, M_V-metallicity, and mass-metallicity relations from §§2-5 with a pulsation equation to predict the temperature-([Fe/H]) relation at the FBE. Temperatures are transformed to $(B\text{-}V)_o$ colors in §7 using an adopted color-metallicity-temperature calibration.

The predicted color-metallicity relation is compared in §8 with the observed $(B\text{-}V)_o$ colors for both field and cluster RRL.

In §9 we turn the problem around by using the new correlations of period, temperature, and mass at the FBE to predict the RRL luminosity, again from the pulsation equation using a new temperature variation at the FBE that has been fitted empirically here to the observational data, rather than using the predicted variation in §§6 & 7.

Section 10 contains a discussion of the observed difference in the zero-point of the log period-([Fe/H]) envelope locus (Figs. 1-4) between field and cluster variables, and the presence or absence of the Oosterhoff period gap in the cluster and the field star samples, respectively, in terms of a proposed different formation history of the samples.

Eight research points made in this paper are summarized in §11.

2. THE DISTRIBUTION OF METALLICITY WITH PERIOD FOR THE 302 FIELD RR LYRAE VARIABLES IN LAYDEN'S SAMPLE

In the 1993 study (S93a), I had used the correlation of mean period with metallicity for 110 field RR Lyraes for which Blanco (1992) had determined improved E(B-V) reddenings. He also had homogenized the existing [Fe/H] metallicity values based on Butler's (1975) calibration of the Preston ΔS metallicity parameter. The Blanco-Butler [Fe/H] scale averages 0.28 dex more metal rich than the globular cluster scale of Zinn and West (1984). I had used the two different metallicity scales, one for the field variables and the other for the clusters, although I had transformed the Blanco-Butler scale to that of Zinn and West. Nevertheless, the field star log P-[Fe/H] diagrams were kept on the Blanco-Butler system, which, at times was inconvenient.

This inconvenience is overcome here, and the sample of field stars has been increased by a factor of three by using the more recent data base of Layden (1994, 1995) which is on the Zinn-West metallicity scale. Layden measured metallicities for his complete sample of 302 RRab Lyrae field variables whose Galactic latitudes are more than $\pm 10^0$, and whose apparent magnitudes are brighter than $\langle V \rangle = 13.5$. Layden's list is from the Fourth Edition of the General Catalog of Variable Stars (Kholopov 1985).

The log P-[Fe/H] distribution for Layden's field star sample is shown in Figure 1. A linear envelope line is drawn by eye as the locus of the shortest period variables at a given [Fe/H] value. This would define the period at the fundamental blue edge of the instability strip if there is no "hysteresis" within in a possible "either-or" transition zone for evolution tracks between the fundamental and first overtone variables. The equation of the envelope line in Fig. 1 is

$$\log P = -0.484 - 0.074([Fe/H]). \tag{1}$$

Editor: Place Figure 1 here

The mid-point ridge line, shown as a dashed line in Fig. 1, is found by averaging the log P values in narrow intervals of [Fe/H]. The data are listed in Table 1. The equation of this line is,

$$\log P = -0.416 - 0.098([Fe/H]). \tag{2}$$

Also listed in Table 1 are the mean (B-V)$_o$ colors within each metallicity bin, calculated from the photoelectric summary of individual colors listed in column 5 of Nikolov, Buchantsova, and Frolov (1984, hereafter the Sophia Catalog), using the reddening corrections for each star based on the absorptions (divided by 3) measured by Layden (1994).

The linear fit (the solid line) to the shortest period envelope data in Fig. 1 is good,

but not perfect. A better fit is achieved for metallicities smaller than -1.8 by bending the envelope toward longer periods. The straight lines in Fig. 2 have the equations, put by eye, of,

$$\log P = -0.484 - 0.074([Fe/H]), \tag{3}$$

for [Fe/H]) more metal rich than -1.8, and two dashed lines whose equations are

$$\log P = -0.610 - 0.144([Fe/H]), \tag{4}$$

and

$$\log P = -0.680 - 0.183(Fe/H]) \tag{4'}$$

for [Fe/H]) more metal poor than -1.8. Equation (3) is the same as Eq. (1) but its application stops for [Fe/H] smaller than -1.8.

Editor: Place Figure 2 here

A still better fit is the continuous parabolic envelope over the entire metallicity range from zero to -2.4 shown in Fig. 3, whose equation is,

$$\log P = -0.452 + 0.033([Fe/H])^2, \tag{5}$$

used previously for a different purpose (Sandage 2004, Fig. 5) using a subset of the present field star data.

Editor: Place Figure 3

These various envelope lines will be used in §6 for the predictions of the temperature at the FBE.

3. THE PERIOD DISTRIBUTIONS FOR DIFFERENT METALLICITIES FOR RRL IN GLOBULAR CLUSTERS

Although the number of stars (302) in Figs. 1-3 is sufficient to show the *continuous* variation of mean period with metallicity (rather than a dichotomy into two period groups), nevertheless it is not yet sufficient to define the position of the short period envelope at the low metallicity end for [Fe/H] < -2 with precision. A larger sample of RR Lyrae variables is needed and is available in globular clusters. The earlier sample from the Third Catalog of cluster variables by Sawyer Hogg (1973) was used in S93a for this purpose.

We have repeated the log period-metallicity diagram for the globular cluster variables in Fig. 4, increasing the cluster sample from 760 stars used by S93a to 919 here by adding

the new variables listed in the 2001 updated catalog by Clemment (2001) cited earlier. The metallicity scale is that of Zinn and West, taken from the listing in the catalogs of Harris (1996). The parabolic envelope of equation (5) is overlaid on the data to compare the cluster data with the field star data in §2 (Figs. 1-3).

Editor: Place Figure 4 here

Two significant differences are evident by comparing Fig. 4 for the cluster variables with Figs. 1-3 for the field variables.

(1). The gap in the [Fe/H] distribution (that is, in the vertical distribution of points) in Fig. 4 between [Fe/H] of -1.7 and -2.0 for the cluster variables is absent in Figs. 1-3 for Layden's field variables. It is this gap that makes the Oosterhoff *dichotomy* into two discrete period groups so evident, partially masking a *continuous* variation of mean periods with metallicity.

(2). The parabolic envelope that fits the short period boundary of the distribution of periods for the field variables in Fig. 3 fails to fit the data for the globular cluster variables. The cluster variables have longer periods at the envelope edge by Δlog P $\sim$ 0.029 dex compared with equation (5). The difference has a significance of about 4 sigma.

There are several possibilities for explaining these two differences between field and cluster variables.

Point (1). The very few variables in the cluster sample in Fig. 4 between [Fe/H] = -1.7 and -2.0 is due, as is well known, to the details of the morphology of cluster horizontal branches through the instability strip in this metallicity range. Most clusters with intermediate metallicities with -1.3 > [Fe/H] > -1.7 have horizontal branches well populated on both sides of the RR Lyrae instability strip, whereas clusters with [Fe/H] between -1.7 and -2.0 produce very few variables because the HB does not penetrate the instability strip.

Clearly, the absence of this Oosterhoff period gap in the field variables shows that the morphology of the horizontal branch of the field RRL *must* differ fundamentally from that in globular clusters in this metallicity range.

The reasons are not presently understood, but a hint may be the variation of the HB morphology with metallicity of the highly unusual globular clusters NGC 6388 and NGC 6441 (Rich 1997 et al.; Pritzl et al. 2000, 2001) where the HB penetrates the instability strip despite its high metal abundance of [Fe/H] $\sim$ -0.5. This behavior is contrary to the horizontal branches of "normal" globular clusters such as 47 Tuc, and the clump HBs of high metallicity galactic clusters. Evidently, there is some parameter-variation (such as the value of the core He abundance, the core mass, variations in deep mixing, etc.) in these two highly

abnormal globular clusters that causes the HB morphology to differ from that of most other of the clusters in the Galaxy.

Point (2). The observed period difference of 0.029 dex between cluster and field variables at the FBE can be accomplished in several ways from the pulsation Eq. (16) in §5. Among them is a luminosity difference of Δlog L = 0.027 at constant temperature and mass, or a temperature difference of Δlog T_e = 0.007 at constant L and mass, or a mass difference of Δlog mass = 0.034 at constant L and T_e, or combinations of each. It need only be recalled that Gratton (1998) has already discussed the possibility that there may be "a real difference between the luminosity of the horizontal branch for clusters and the field".

Point (3). A third possibility is that the metallicity scale due to Layden (1994) in Figs. 1-3 for the field variables is not the same as the used by Harris (1996) for the clusters. The difference seen between Figs. 1-3 and Fig. 4 would disappear if the field points in Figs.1-3 were moved downward by Δ[Fe/H] $\sim$ 0.3 dex, or if the cluster data were made more metal poor by the same amount. But no systematic shifts by this amount are possible if the statements by both Layden and by Harris are correct that their scales are both tied to the scale of Zinn and West (1984).

4. SELECTED RECENT ABSOLUTE MAGNITUDE CALIBRATIONS OF RR LYRAE VARIABLES AS A FUNCTION OF [Fe/H]

Many calibrations, both observational and theoretical, of RR Lyrae luminosities as functions of metallicity have been made since the linear calibration via the pulsation equation was made in S93a.

All of the second and third generation theoretical models for the position of the *zero-age* horizontal branches show that the relation between $M_{\rm bol}$ (and hence closely M_V) and [Fe/H] must be non linear, i.e. the branch loci of the ZAHB tracks are more closely stacked in luminosity at the low metallicity end of the distribution than at the high metallicity end, for equal intervals of [Fe/H], even as the low metallicity ZAHBs are brighter than those of high metallicity. Examples, among many, are the models of Lee, Demarque & Zinn (1990); Castellani, Chieffi, & Pulone (1991); Bencivenni et al. (1991); Dorman (1992); Caputo et al. (1993); Caloi, D'Antona & Mazzitelli (1997); Salaris, Degl'Innocenti & Weiss (1997); Cassisi et al. (1999); Demarque et al. (2000); VandenBerg et al. (2000, Figs. 2, 3, and 20); Catelan, Pritzl, & Smith (2004). A graphical summary showing several of the predicted M_V(HB)-[Fe/H] relations derived from these models is given by Cacciari & Clementini (2004).

Observational and/or semi-theoretical calibrations that also show the need for a non-

linear M_V([Fe/H]) relation are, among others, the studies by Caputo (1997); Gratton et al. (1997): De Santis & Cassisi (1999, Fig. 15), Caputo et al. (2000), and McNamara et al. (2004).

We use several of these calibrations in the pulsation equation to predict the temperature at the FBE of the instability strip in the next section, replacing the linear calibration derived in S93b of,

$$M_V = 0.94 + 0.30([Fe/H]). \tag{6}$$

We use the non-linear calibrations of Caputo et al. (2000), Catelan et al. (2004), and McNamara et al. (2004) from their tie-in to Delta Scuti stars, and the linear calibration of Clementini et al. (2003) from their calibration via the RR Lyrae stars in the LMC. The equations are assumed to be as follows.

We have approximated the graphical representation of the calibration of Caputo et al. (2000, their Fig. 2a) by a parabola, as,

$$M_V = 1.576 + 1.068([Fe/H]) + 0.242(Fe/H])^2. \tag{7}$$

Using $M_{\rm bol}$ = M_V + BC, with BC = 0.06 +0.06 ([Fe/H]), and $M_{\rm bol}$(sun) = 4.75, it follows from (7) that

$$\text{Log}L_{\rm bol} = 1.245 - 0.451([Fe/H]) - 0.097([Fe/H])^2. \tag{8}$$

The adopted bolometric correction here is the same as was used by Sandage and Cacciari (1990), justified there. The tables by Bell and Tripicco in Sandage et al. (1999, Table 6) show, of course, that the BC varies also with temperature and atmospheric turbulent velocity as well as with metallicity. Interpolation within the tables for turbulent velocity of 5 km s^{-1} at a color of $(B\text{-}V)^0$ = 0.24 (which is close to the blue edge) gives BC = 0.05 + 0.06([Fe/H]). Using a turbulent velocity of 1.7 km s^{-1} gives BC = 0.06 +0.069 ([Fe/H]), again at $(B\text{-}V)^0$ = 0.24. These justify our continued use of 0.06 + 0.06 ([Fe/H]) here.

The calibration equations from the theoretical models of the ZAHB by Catelan et al. (2004) using an oxygen enhancement of [alpha/Fe] = 0.3 and [Fe/H] = [M/H] - 0.213 give,

$$M_V = 1.179 + 0.548(Fe/H]) + 0.108([Fe/H])^2, \tag{9}$$

from their Eq. (12) after some reduction to change [M/H] into [Fe/H]. This transforms in the same way as above to

$$\log L_{\rm bol} = 1.404 - 0.243([Fe/H]) - 0.043(Fe/H])^2. \tag{10}$$

The linear calibration of Clementini et al. (2003) using the observed RR Lyraes in the LMC and an adopted LMC modulus of (m-M) = 18.54 gives,

$$M_V = 0.845 + 0.214([Fe/H]), \tag{11}$$

or,

$$\log L_{\rm bol} = 1.538 - 0.110(Fe/H]). \tag{12}$$

Equations (11) and (12) refer to the mean (evolved) HB. To change to the level of the ZAHB we must make the equations fainter by about 0.1 mag in V, or 0.025 in log L (S90a).

The equations for the two-line calibration of McNamara et al. (2004) are; M_V = 0.50 independent of [Fe/H] for metallicities more metal poor than -1.5, and M_V = 1.13 + 0.42 ([Fe/H]) for [Fe/H] between -0.5 and -1.5.

These transform to

$$\log L_{\rm bol} = 1.676 - 0.024([Fe/H]), \tag{13}$$

for [Fe/H] < -1.5, and,

$$\mathrm{Log} L_{\rm bol} = 1.424 - 0.192([Fe/H]), \tag{14}$$

for [Fe/H]) > -1.5.

5. THE DEPENDENCE OF RR LYRAE MASS ON METALLICITY

To make the calculation of T_e(FBE) from the pulsation equation, we also need the mass as a function of metallicity. In S93b, I adopted the ZAHB calculation of RR Lyrae mass at log T_e = 3.85 by Dorman (1992) as log mass = -0.288 - 0.059 ([Fe/H]), where he had used enhanced oxygen abundances and modern opacity tables. More recently this theoretical calculation of RR Lyrae masses has been verified and extended by Bono et al. (1997a), again using enhanced oxygen abundances and the latest opacity tables cited by them. The resulting masses on the ZAHB at log T = 3.85 are listed in Table 2 of Caputo et al. (2000), and are adopted here. The resulting linear mass equation over the relevant metallicity range is,

$$\mathrm{Logmass} = -0.283 - 0.066([Fe/H]), \tag{15}$$

which we adopt. This deviates by not more than 0.02 dex in mass from Dorman (1992) over the metallicity range from 0 to -2.5.

Confirmation that the mass of metal poor RR Lyraes is larger than that for metal rich variables is available from analyses of the observations of double mode variables via the

Peterson (1973) diagram and the subsequent calculations by Peterson (1978, 1979), Cox et al. (1980), Cox et al. (1983), and Cox (1987) and references therein. The calculations by Kovacs et al. (1992) that show the sensitivity of the results to various chemical composition mixtures are illustrated in Fig. 4 of S93b.

The masses from Eq. (15) are for the ZAHB at log $T_e = 3.85$. They will not be precise even at this fixed temperature if evolution brings stars from different parts of the HB into the instability strip. We neglect the detail in this reconnaissance study; it does not change the sense of the argument that follows in Figs. 5 & 6 of the next section.

6. PREDICTED VARIATION OF TEMPERATURE WITH METALLICITY AT THE FUNDAMENTAL BLUE EDGE

Many new versions of the pulsation equation have been calculated since the pioneering paper by van Albada and Baker (1973) (eg. Chiosi et al. 1992; Simon & Clement 1993; Bono et al. 1997b with earlier references), but each give nearly identical dependencies of period on temperature, luminosity, and mass. We continue to use the van Albada and Baker formulation here.

Their equation, transposed to make temperature the independent variable, is

$$\log T_e = 0.241 \log L - 0.287 \log P - 0.196 \log M + 3.304. \tag{16}$$

If the dependencies of L, P, and mass on metallicity have been expressed as relations at the FBE of the instability strip, either on the ZAHB or on the mean HB as evolved from the ZAHB, then Eq. (16) will give the temperature at that edge. We make the assumption here that the HB is truly horizontal in V magnitudes and, therefore, that equations (8), (10), (12), (13), and (14) also define the bolometric luminosity at the blue fundamental edge as well as at the mean strip position to which many of the luminosity calibrations of the aforesaid equations apply. This is a fully adequate approximation for the restricted purpose of this paper which is only to show the *need* to invoke a variable temperature with metallicity at the FBE of the strip rather than to finalize a definitive determination of it.

Indeed, uncertainties presently exist in the temperature- color calibration (§7) at the level of 0.02 mag in B-V. Similar uncertainties also exist at the 0.02 mag level in the observational data for the B-V color at the FBE edge due to uncertainties in the reddening. In addition, theoretical uncertainties exist in the constants of the pulsation equation including its zero point [i.e. 3.304 in Eq. (16)]. These all conspire against a definitive “final” calculation of T_e(BFE). Nevertheless, all log L calibrations to date, and all P-([Fe/H]) displays such

as in Figs. 1-4, require the same qualitative variation of T_e and color of the fundamental blue edge with metallicity which is the purpose of this paper, which we now demonstrate.

To illustrate the nature of the 30 solutions for T_e in the completely filled log P([Fe/H]) and log L([Fe/H]) parameter space, it is sufficient to choose only a subset of the P([Fe/H]) and L([Fe/H]) combinations. Here the subsets are divided into two groups. In the first we keep the luminosity calibration fixed using Eq. (10) by Catelan et al. (2004), and use with it the four different log P-metallicity envelopes from Figs. 1-3. These loci are (a) the log P([Fe/H]) envelope in Eq. (1) as in Fig. 1; (b) the three-line envelopes of Eqs. (3), (4) and (4') in Fig. 2; and (c) the parabolic envelope of Eq. (5) in Fig. 3.

Inserting the Catelan et al. (2004) log L([Fe/H]) relation from equation (10), the Bono et al. (1997a) mass equation from Eq. (15), and the log P([Fe/H]) relations from Eqs. (1), (3), (4), (4') and (5) into the pulsation equation (16) gives the run of predicted log T_e with [Fe/H] shown in Fig. 5. The relation using the midpoint correlation of [Fe/H] with period [Eq. (2)] is also shown.

Editor: Place Figure 5 here

As an example, the predicted log T_e relations at the FBE using the parabolic envelope line of Eq. (5), the Bono mass Eq. (15), and the Catelan et al. luminosity calibration of Eq. (10) is,

$$\log T_e(FBE) = 3.827 - 0.046([Fe/H) - 0.019([Fe/H])^2, \tag{17}$$

shown in Fig. 5 as the dashed line marked number 3.

Alternatively, by keeping the envelope log P([Fe/H]) relation fixed using Eq. (5) for the parabolic fit, and using five different Log L(Fe/H]) calibrations give the predicted run of log T_e shown in Fig. 6.

Editor: Place Figure 6 here

The characteristics of all the solutions in both diagrams is that the predicted temperature at the fundamental blue edge varies with [Fe/H], first becoming hotter as [Fe/H] weakens from 0 to within the range of -1.2 to -1.5, and then cools again for still decreasing metal abundance. At no metallicity is it constant at the FBE with varying [Fe/H], although its variation is less than Δlog $T_e = 0.01$ between [Fe/H] of -0.5 and -2.0 along any given line of fixed luminosity calibration.

7. TRANSFORMATION OF THE TEMPERATURE VARIATION AT THE FBE TO B-V COLORS

A number of new calibrations of how B-V color varies with log T_e, metallicity, surface gravity, and atmospheric turbulent velocity have been made since the relation, taken from an unpublished calibration of Bell, as quoted by Butler et al. (1978, their Fig. 11), was used by S93b (Eq. 4 there). Six of these modern calibrations have been compared by Cacciari, Corwin, & Carney (2004, their Fig. 7). The total differences between the various calibrations in the predicted B-V colors at a given temperature near 7000 K (log T = 3.845) is large at 0.08 mag. Or read the other way, at a color of B-V = 0.28, the temperatures range between 6950 K (log T_e = 3.842) to 6400 K (log T = 3.806) for the calibrations that are compared by Cacciari et al. (2004).

The hottest calibrations for a given color are those of Sandage, Bell, and Tripicco (1999, hereafter SBT) and Castelli (1999). The coolest is that of Montegriffio et al. (1998). Intermediate are the calibrations of Carney, Storm, & Jones (1992), and Sekiguchi & Fukugita (2000). The bulk of the comparisons show a smaller spread of 0.04 mag in B-V between the calibrations of SBT, SF, and CSJ.

We adopt the intermediate calibration of CSJ (1992, their Eq. 13), which, in the temperature range of interest (log T_e between 3.85 and 3.80), can be put with sufficient accuracy into the logarithmic form rather than as function of 5040/T as they give it, to be,

$$(B-V) = -2.632 \log T_e + 0.038([Fe/H]) + 10.423, \tag{18}$$

in the interval 0.20 < B-V < 0.30.

Comparison between the SBT and the SF scales read at the fixed color of B-V = 0.24 at [Fe/H/] = -1.5 (near the mid range of the relevant parameter space), give log T_e = 3.848 (T_e = 7046 K) for CSJ from eq. (18), 3.857 (T_e = 7194 K) for SBT, and 3.852 (T_e = 7112 K) from SF. Hence, the temperatures on the three scales differ by Δlog T_e = 0.009 at B-V = 0.24.

The coefficient of [Fe/H] in Eq. (18) is, of course, a strong function of temperature, increasing due to Fraunhofer blanketing and atmospheric backwarming with decreasing temperature. The value of 0.038 in Eq. (18) is a compromise between 0.026 at B-V = 0.24 for the SBT models (interpolating in their Table 6) and 0.047 in the SF calibration, a value that is surely too large at the hot temperature corresponding to B-V = 0.24.

Using Eq. (18) we transform the T_e at the FBE for each of the equations that generate the family of curves in Figs. 5 and 6 into the predicted run of B-V colors with metallicity at the FBE.

To illustrate one equation of the family we insert the base-line parabolic equation for the log P([Fe/H]) envelope relation of Eq. (5) and the Catelan et al. luminosity calibration of Eq. (10) into Eq. (18) to obtain the predicted run of B-V color at the FBE for that combination as,

$$(B-V)_{\mathrm{FBE}} = 0.35 + 0.159([Fe/H]) + 0.050(Fe/H])^2, \tag{19}$$

which is the dashed line 3 in Fig. 7.

The complete sets of the families from Figs. 5 and 6, but now in B-V, are shown in Figs. 7 and 8.

Editor: Place Figures 7 and 8 here

All curves in Figs. 7 and 8 have the same character. Each predicts a bluing as [Fe/H] decreases from 0 to about -1.5, after which the predicted color becomes redder. Over the relevant range of metallicities from [Fe/H] = -0.9 to -2.2, which contains most of the Galactic globular clusters, the color change is only Δ(B-V) ∼ 0.02 mag.

We emphasize that the zero points of the B-V values in Figs. 7 and 8 have not been adjusted to conform with observational data. They are the calculated from the theoretical zero points in the several relevant equations. Given the range of errors in each of these equations, it is remarkable that the agreement of the predicted color variation with the observations, to be discussed in the next section, is so good.

8. COMPARISON OF PREDICTED AND OBSERVED B-V COLORS OF FIELD AND CLUSTER VARIABLES AT THE FUNDAMENTAL BLUE EDGE

8.1. Which definition of mean color to use?

Which definition of "mean color", averaged over the light curve, best approximates the color of an equivalent static star? Three definitions are used in the literature, defined by the following operational procedures. (1) Change B and V magnitudes into intensity units and average over the light curve, calculating mean values of $\langle B\rangle_{\mathrm{int}}$ and $\langle V\rangle_{\mathrm{int}}$, changed back to magnitude units, and then subtract to form the color $\langle B\rangle_{\mathrm{int}}$ - $\langle V\rangle_{\mathrm{int}}$. (2) Change the color curve in B-V from magnitude to intensity units and average over the intensity color curve, changed back to magnitude units to form $\langle B-V\rangle_{\mathrm{int}}$ (3) Keep the color curve in magnitude units and integrate over the cycle to obtain $(B-V)_{\mathrm{mag}}$.

These procedures give colors that can differ by as much as 0.05 mag for highly asym-

metric light and color curves of high amplitude. Which is correct to give an approximation to the color of a "static star" with the same average energy output?

In a semi-analytical treatment, Preston (1961) showed that the best estimate of the color of such a static star is $(B-V)_{\rm mag}$. I reached the same conclusion (S90a) in a semi-empirical discussion based on the calculated and observed slopes of the period-color relation calculated from the pulsation equation, choosing a color equivalent definition that made the predicted and observed slopes the same. Corwin and Carney (2001) also concluded that $(B-V)_{\rm mag}$ was the appropriate color to use, reversing a previous discussion by Carney, Storm, and Jones (1992) to the contrary. A definitive theoretical discussion by Bono, Caputo, & Stellingwerf (1995) showed that $(B-V)_{\rm mag}$ is within 0.01 mag of $(B-V)_{\rm static}$ for all blue amplitudes smaller than 1.6 mag. A table of differences between the three types of color definitions and $(B-V)_{\rm static}$, which they calculated, is given by them.

We use $(B-V)_{\rm mag}$ in the remainder of the paper. We have converted other listings in the literature to $(B-V)_{\rm mag}$ where they differ, either by using Table 4 of Bono et al. (1995), or using the ΔC(A) correction formulation in S90a. A detailed reading of the literature is often required to determine which mean color definition has been used by particular authors.

8.2. Observed $(B-V)^0_{\rm mag}$ for a sample of field variables

We have attempted to assemble a data base of reddening- corrected $(B-V)^0$ colors of RR Lyrae variables accurate at the 0.02 mag level for both field and clusters variables. If the observational data are from a variety of observers, they must be reduced to a common photometric standard system, taking out systematic zero-point differences between the sets. In addition, a uniform definition of what kind of mean color, as just discussed, must be used. More uncertain are the corrections for E(B-V) reddening, that themselves are generally be accurate only to within 0.02 mag. Hence, detection of the relatively small color variations with [Fe/H] predicted in Figs. 7 and 8 is near the limit of accuracy of the data now available.

A large list of observed photoelectric colors for field RR Lyrae variables is in the catalog by Nikolov, Buchantsova, & Frolov (1984), hereafter referred as the Sofia Catalog. Nine photoelectric data sets from the literature were compared and reduced to a common system, producing a highly homogeneous list of $(B-V)_{\rm mag}$ colors for 210 variables in that catalog (their Table 2, column 2). The photoelectric data, so reduced, are from Fitch et al. (1966), Sturch (1966), Clube et al. (1969), Paczynski (1965a,b, 1966), Stepien (1972), Epstein (1969), Lub (1979), Preston & Paczynski (1964), and Kinman (1961).

I have used the listings in the Sophia catalog and corrected them for reddening by using

the homogeneous set of absorption values in V measured by Layden (1994), using E(B-V) = A(V)/3.0 for all stars in common with the Sophia catalog and the Layden list. In this way, $(B-V)_o$ colors were obtained for 142 field RR Lyraes in the Layden sample, plus 10 additional from Blanco's study discussed in S93a but not in Layden's list, and an additional 8 from Lub that are not in Layden but reduced to his absorption system by cross checking the Lub list as constructed in S90a with the Layden list. A total of 160 field variables with $(B-V)_o$ colors are available in this way. The color values are not listed here because they can be readily obtained from the same original sources.

Editor: Place Figure 9 here

The colors for these field variables are plotted in Fig. 9 vs. Layden's [Fe/H] metallicities. As emphasized earlier, the [Fe/H] values are on the system of Zinn and West (1984). The line is equation (19), which is the prediction of T_e using the pulsation equation (16) and the transformation to B-V via Eq. (18). It is the predicted color-metallicity locus at the FBE using the Catelan et al. (2004) luminosity calibration of the FBE in Eq. (10) and the parabolic envelope locus to the period- metallicity relation of Eq. (5) in the pulsation equation for T_e, transformed to B-V via Eq. (18). The drawn line is repeated from Figs. 7 and 8, which is one of the curves in the family shown there.

No adjustment of the *zero point* of the theoretical equation (19) to fit the observations has been made in Fig. 9. Hence, as stated earlier, the generally good agreement of this calculated curve with the observations of the bluest color at a given metallicity is remarkable because the various zero points in the theoretical and the observed equations used for the prediction have been left as they had been previously calculated.

The predicted T_e([Fe/H]) line in Fig. 9 fits the observations tolerably well except for metallicities more metal poor than [Fe/H] = -2.0 where it does not bend sufficiently toward redder colors. A better representation is derived in the next section (Fig. 11 there) where the color data for variables in globular clusters are combined with these field star colors.

8.3. The Observed $(B-V)^0_{\rm mag}$ Colors for Globular Cluster RRab Lyrae Variables From the Literature CCD Photometry

The globular cluster color data are set out in Fig. 10. They have been taken from the literature, either from modern CCD photometry, or from reliable pg photometry. The literature citations for the 21 clusters are listed in Table 2. Most data have been transformed to the $(B-V)_{\rm mag}$ mean color system by Table 4 of Bono et al. (1995). However, if the original data were originally listed as $(B-V)_{\rm static}$, they were kept at that because, according

to Bono et al., the "static star" color is within 0.01 mag of $(B-V)_{\rm mag}$ for all amplitudes of interest.

Editor: Place Figure 10 here.

The E(B-V) reddening values determined by the original authors have been replaced by the homogeneous values listed by Harris (1996), except for NGC 4590 where the value proposed by Walker (1994) is obviously more correct.

Editor: Place Figure 11 here.

The data in Figs. 9 and 10 are combined in Fig. 11. Although there are outriders to the bulk of the distribution at blue colors, the trend is for the clusters with [Fe/H] between -1.0 and -1.7 to be bluer at the short period edge than either for the more metal rich or the more metal poor variables, similar to the solid curves in Figs. 9 and 10. A stronger bend toward the red is drawn as a new curve fitted empirically to the data for [Fe/H] < -2.0 in Fig. 11. It is a slightly better fit to the combined data than the curve that is drawn in Fig. 9 and 10 using Eq. (19). The equation of this empirical curve is,

$$B-V = 0.351 + 0.172([Fe/H]) + 0.061([Fe/H])^2 \tag{20}$$

This can be transformed to temperature via Eq. (18) to give

$$logT_e = 3.827 - 0.051([Fe/H]) - 0.023([Fe/H])^2 \tag{21}$$

We aver that this applies at the FBE because we have assumed that the blue envelope loci in Figs. 3 and 10 (solid line) refer to that edge.

9. THE PROBLEM TURNED AROUND TO PRODUCE A NEW LUMINOSITY CALIBRATION

We now repeat the calculation of the luminosity calibration with metallicity made in S93a but here we use the new correlations between period, temperature, and mass relations with metallicity set out in the previous sections. The method is to insert the parabolic Eq. (5) for the period-metallicity locus at the FBE, the new semi-empirical equation for the temperature at that edge from Eq. (21), Fig. 11, and the mass-metallicity relation from Eq. (15) into the pulsation equation, permitting the calculation of the luminosity.

Using Eqs. (21), (5), and (15) in Eq. (16) gives,

$$logL_{\rm bol} = 1.401 - 0.264(Fe/H]) - 0.056([Fe/H])^2. \tag{22}$$

As before, using M_{bol} = -2.5 log L + 4.75 and BC = 0.06 + 0.06 ([Fe/H]) in $M_V = M_{bol}$ - BC gives, from Eq. (22),

$$M_V = 1.187 + 0.600([Fe/H]) + 0.140(Fe/H])^2, \quad (23)$$

over the metallicity range of [Fe/H] $\sim$ -0.5 to -2.3. This calibration updates the linear calibration of Eq. (6) given in S93b, made by the same method, but using the new assumptions here that relate period, mass, and temperature variations with metallicity.

As already said several times, the zero point in equation (23) is the theoretical value based on the zero points adopted in each of the pulsation, mass, and color-temperature equations. Because we cannot guarantee that these combined zero points are precise, we change the theoretical zero point in Eq. (23) to conform with the independent data on M_V (RR) determined empirically. Clementini et al. (2003) have measured the mean apparent magnitude of RRLs in the LMC as a function of [Fe/H], which can be changed to absolute magnitude by assuming a distance modulus of the LMC determined by other means. They adopt $(m\text{-}M)_o$ = 18.54 based on an adopted P-L relation of the LMC type I long period Cepheids. However, Tammann, Sandage & Reindl (2003) argued that the Cepheid P-L relation differs between the Galaxy and the LMC, and they fixed the distance modulus the LMC also at $(m - M)_o$ = 18.54 by means other then the long period Cepheids.

The data of Clementini et al. give $\langle V \rangle$ = 19.064 for the RR Lyraes at [Fe/H] = -1.5 in the LMC, which, with the assumed modulus of 18.54, give M_V = 0.524. This differs by 0.078 mag from the zero point in Eq. (23) of M_V = 0.602 for this metallicity. Hence, we must make the zero point in Eq. (23) brighter by 0.078 mag to put it on the observed scale of the Clementini et al.

But the Clementini data refer to the average RR Lyrae apparent magnitude which already accounts for the average luminosity evolution from the ZAHB. A difference of about 0.1 mag is expected between the ZAHB and the average evolved HB level (S93b). Remarkably, this is near the 0.078 mag difference just quoted. It continues as a surprise that the calculated and observed zero points, corrected for evolution, are so nearly the same at the 0.10-0.078 = 0.02 mag level. Again, this can only mean that the zero points of the various relations that go into Eq. (23) are themselves fully compatible with the various observations that comprise them.

Therefore, our final calibration of the ZAHB using the theoreticians route via the pulsation equation, but zero-pointed through the LMC as in Eq. (23) and made brighter by 0.078 mag, is,

$$M_V = 1.109 + 0.600([Fe/H]) + 0.140([Fe/H])^2, \quad (24)$$

valid for the average evolved HB at the FBE.

10. IS THERE A DIFFERENCE BETWEEN FIELD RR LYRAES AND THOSE IN CLUSTERS?

It remains to discuss the significant of the difference between Layden's field star sample and the RRLs in clusters in the absence of the Oosterhoff gap in Fig. 1 and its presence in Fig. 4, and, in addition, in the shift of the short period envelope lines between of Figs. 1 and 4 in the period-metallicity correlations. Both differences were set out earlier in §3.

The absence of a gap (i.e. the presence of a continuum) in particular Galaxian samples of field RRLs had already been seen in the original period-metallicity sample of Preston (1959, his Fig. 4). It is also highly manifest in the much larger sample of Layden (1994, 1995) in Figs. 1-3 here. The gap is also absent in recent discovery surveys of faint RRL in high latitudes (eg. Vivas & Zinn 2002, 2004), A summary of the relevant evidence is by Catelan (2004)[1]

Even more to the point, for some samples of the dwarf spheroidal companions to the Galaxy the consequence of the intermediate value of the mean period, $\langle P \rangle$, is that there is no Oosterhoff separation into a *dichotomy* for different metallicitues (Bono, Caputo, & Stellingwerf 1994; Mackey and Gilmore 2003 ; Mateo 1996; Pritzl et al. 2002; Cseresnjes 2001; Clementini et al. (2004); and Dall'Ora et al. (2003). The result is that the mean periods of the RRL are *intermediate* between the two Oosterhoff groups in the Galaxy (Catalan 2004, Table 1; Siegel & Majewski 2000, their Fig. 6). Why?

The general morphology-metallicity progression for horizontal branches in the globular clusters in the Galaxy is this. The HBs in the high metallicity clusters for [Fe/H] $\gtrsim -0.7$ do not penetrate the instability strip because they are redder than the strip color boundaries. Hence, such clusters contain few if any RR Lyrae variables. The prototype example is 47 Tuc.

A counter example in the opposite sense is NGC 7006 which has an abnormally red segment to its HB for its metallicity (Sandage & Wildey 1967), yet it contains many RRLs. Also in an opposite sense (abnormally blue HB for its metallicity) is M13 where the branch misses the instability strip altogether because of its excessive blueness, yet its metallicity is nearly identical with that of M3 which contains many variables (cf. Cho et al. 2005 for a modern comparison of M3 and M13).

Hence, the cluster morphology-metallicity relation that is responsible for the Oosterhoff

---

[1]However, contrary evidence exists showing the presence of the gap in the faint field RRL samples of Suntzeff, Kinman, and Kraft [1991], in contrast to Figs. 1-3 and to the results of Vivas & Zinn (2002, 2004). Catelan (2004) remarks that "the reason for the discrepancy between the two studies is unclear at present."

gap in the Galaxy is not perfectly consistent. The most extreme examples of this second parameter effect are the metal rich ([Fe/H] $\sim$ -0.50) clusters NGC 6388 and NGC 6441 which have abnormally long periods for their amplitudes (Pritzl et al. 2000, 2001), yet both have abnormally blue extended horizontal branches never before seen in other high metallicity clusters (Rich et al. 1997). The globular cluster M2 is a less extreme example (Lee & Carney 1999b) with much longer periods for a given amplitude. Also, similar to M2, the second- parameter custer NGC 5986 (Alves, Bond, & Onken 2001) has a period-amplitude diagram with abnormally long periods compared with even Oosterhoff II clusters, although the metal abundance is only -1.58 on the Zinn & West system. Its HB is abnormally blue, as in M13 (van den Bergh 1967), for this metallicity. This is opposite the sense of the effect in NGC 7006.

Although not yet conclusively proved, the reasons for such behavior is currently suspected to be different chemical composition effects that control the details of the HB morphology (eg. variations in the helium core mass, differences in the mass loss from the AGB to the HB, differences in the deep mixing etc.). If so, the difference between the field and the cluster RR Lyraes (Figs. 1 and 4) would suggest that these field variables have had a different history in their chemical evolution than those in clusters. Yes, but why?

Suppose that the bulk of the field RRLs have come from the disintegration of dwarf spheroidals that once were companions to the Galaxy but have since been accreated and disrupted. This is almost certainly proved now by the discovery of the discrete RRL streams in the Sloan survey for high latitude variables (Ivezic et al. 2000; Yanny et al. 2000; Newberg et al. 2002), and the similar discovery by Vivas et al. (2001 cf. also Vivas & Zinn, 2002, 2004) from the Venezuela QUEST survey. These discrete streams, widely assumed to be debris from original dwarf spheroidal companions to the Galaxy, now disrupted, are the generalization of the many high velocity moving groups discovered by Eggen (1977), the first of which was the Grombridge 1830 group that contains RR Lyrae itself (Eggen & Sandage 1959). The Sloan survey, and other evidence before it (eg. Freeman 1987; Majewski 1993; Lynden-Bell & Lynden Bell 1995; Freeman & Bland-Hawthorn 2002), showed that the Eggen high velocity moving groups are real. The disruption of dwarf spheroidal Galaxian companions is seen directly today in the Sagittarius disintegrating dwarf (Ibata, Gilmore, & Irwin 1994, 1995) as it is being torn apart by tidal interaction with the Galaxy.

It is known that the chemical evolution of the individual dwarf spheroidals differ, depending on their individaual luminosity, i.e. mass (eg. Aaronson 1986; Skillman et al. 1989, Caldwell et al. 1998; Mateo 1998, his Fig. 7 for a summary). Hence, the HB morphology of the products of the disruption (among which are the halo RRLs), should also differ by second-parameter effects. In particular, as a group, they should differ from the "normal"

HB morphology of Galactic globular clusters where the chemical evolution has gone further toward "completion" because the much higher mass of the Galaxy means stronger gravity and therefore the chemical products of AGB nucleosynthesis can be retained, unlike the situation in the dwarf spheroidals where supernovae winds can cause mass loss from the parent dwarf.

Because of the variable ability of the parent galaxies to retain the products of the chemical build up, depending on the mass, the chemical evolution of the parent dwarf spheroidals has differed from that history for most of the globular clusters in the Galaxy that have the normal Oosterhoff gap. Hence, the details of the Oosterhoff effect can be expected to differ.

If so, one can no longer support the canonical idea that the field RR Lyraes have come from the general Galactic globular cluster population, but rather from the previous dwarf spheroidal companions with varying HB morphologies.

The hypothesis to be tested is this. The majority of the globular clusters in the inner Galactic halo have a common origin that coincided with the origin of the bulk of the Galaxy itself (van den Bergh & Mackey 2004). The evidence supports the idea that this process is a more or less coherent collapse, albeit with noise, similar to that of Eggen et al. (1962, ELS; Sandage 1990c) for the lower halo, the bulge, and thin, and thick disks. On the other hand, as argued above, many of the halo field variables have come from the "outside" in a type of Searle-Zinn (1978) bottom-up hierarchical fragmentary build up in some form of the cold dark matter scenario for origins.

However, the most telling argument against the bottom-up build up from fragments of the *bulk* of the Galaxy, and other similar high mass galaxies, is the recent discovery of normal E galaxies at the very large redshifts of $z > 2$ (McCarthy 2004) which would not exist in the hierarchical build-up from small fragments. Rather, there existence is the natural consequence of an ELS-type collapse on time scale short relative to the Hubble time. Said differently, normal E galaxies undergoing passive evolution, but otherwise fully formed, cannot be created by slow hierarchical build up on the cold dark matter scenario, but must be formed very early, very rapidly, all components of a protogalxy having a negative total energy. This is direct ELS.

A test of the different-origins hypothesis for the field and the cluster variables in the Galaxy is to map the morphology- metallicity relation of the HB of the dwarf spheroidals and to match the differences in the period-metallicity envelope, for example, with such second parameter indicators as the period- amplitude relation, the period-rise tine correlation, and the period-color relations with the Oosterhoff period shifts as functions of morphology and metallicity. Such a study is beyond the scope of this paper but is in progress.

11. SUMMARY

There are eight principle research points in this paper.

1. The best fitting envelope of the period-metallicity correlation (Fig. 1) at the shortest periods for the field RR Lyraes in the Layden (1994) sample is non-linear. A parabolic relation [Eq. (5)] more adequately fits the data at low metallicity than the linear envelope adopted earlier (S93a).

2. The shape of the envelope in item 1 is also a good fit to the period-metallicity relation for RRL in globular clusters (Fig. 4), except that it is displaced in zero point toward longer periods by $\Delta \log \mathrm{P} = 0.029 \pm 0.007$. This is another piece of evidence, joining several already in the literature, that the field and cluster variables may have different origins (points 7 and 8 below).

3. The equations for various period-metallicity envelopes in items 1 and 2 are inserted into the pulsation equation, together with a series of new calibrations of the absolute magnitude of RR Lyrae variables, and with an updated calibration of RR Lyrae mass with metallicity, to predict a family of temperature variations at the fundamental blue edge as function of metallicity. All combinations of the input assumptions show that T_e at the FBE varies with metallicity, changing by $\Delta \log \mathrm{T}_e = 0.04$ over the range of ([Fe/H]) between 0 and -2.5. It first becomes hotter as [Fe/H] changes from 0 to -1.5, and then cooler for as the metallicity decreases further (Figs. 5 & 6).

4. The predicted FBE temperatures are transformed into B-V color (Figs. 7 & 8) by the adopted temperature-color relation of Eq. (18). The color variation is predicted to be at the level of 0.03 mag in (B-V) for [Fe/H] between -1.0 and -2.5 for any given choice of the absolute magnitude calibration and of the variation of the period-metallicity locus at the FBE.

5. Comparison of this predicted color variation for both field and cluster variables (Figs. 9 & 10) shows general agreement in the shape of the variation and in the color zero point. The agreement of this theoretical color zero point with the observations is remarkable because the calculations are made adopting the zero points in the pulsation equation [Eq. (16)], the mass equation (15), the color-temperature transformation Eq. (18), and the luminosity calibration equations, each of which have a range of uncertainty.

6. An iteration of the predicted envelope locus for the color-metallicity correlations of Figs. 9 and 10 to better fit the color-[Fe/H] data for metallicities smaller than -2.0 gives the semi-empirical locus of Eq. (20), shown in Fig. 11. This envelope, now made to better fit the observations, is used to make the calculation via the pulsation backward to obtain

an improved absolute magnitude calibration of Eq. (23) which refers to the age zero HB. This equation is then re-zero pointed to refer to the average evolved HB by adopting the Clementini et al. (2003) LMC observation that $\langle V \rangle_o = 19.064$ at [Fe/H] = -1.5 for the LMC RRLs and using the modulus of the LMC as (m-M)$_o$ = 18.54 (Tammann et al. 2003) which does not use the LMC classical Cepheids. This gives a new calibration of the average M_V of the evolved HB of Galactic globular clusters [(Eq. (24)].

7. Returning to the observed offset of the period- metallicity envelopes for the period distributions of the field variables relative to those in clusters (Figs. 1 & 4), and the presence or absence of the Oosterhoff gap in the clusters and in the field, we conclude that the origins of the two groups may be different. The presence in one and absence in the other of the Oosterhoff gap proves that the variation of the morphology of the HB with [Fe/H] differs between the two groups. This is another manifestation of the second parameter effect seen in only a handful of the Galactic globular clusters such as M13, NGC 7006, M2, NGC 5986 and the extreme cases of NGC 6388 and NGC 6441.

We agree with the growing consensus that the origin of at least a subset of the halo variables is the disruption by tidal friction of structures related to the dwarf spheroidals, where it is known that they have varying degrees of chemical evolution- completion depending on their mass (luminosity). It is also known that the Oosterhoff gap characteristics varies among them. This variation is suggested to manifest itself in the difference in the morphology of the HB between the Galaxy and the dwarf spheroidals, similar to the differences seen between the bulk of the Galactic globular clusters and the second parameter clusters such as NGC 6838, NGC 6441, NGC 7006, M2, and NGC 5986.

8. A test of the hypothesis is to study the systematics of the morphology of the dwarf spheroidal HBs and its variation with metallicity. The HB morphology for them is expected to be systematically different from that in the Galaxy, and that difference is postulated to be a function of the mean metallicity. Such a study of comparative HB morphology between the normal and the second parameter globular clusters in the Galaxy and the local dwarf spheroidal companions is beyond the scope of this paper, but has been started.

ACKNOWLEDGEMENTS: An early paper (unpublished), refereed by Geselle Clementini, has been rewritten here with a different goal and emphasis. The many suggestions by Clementini, leading to the old problems being analyzed from a new direction, are gratefully acknowledged. Other comments on the original paper by Fillipina Caputo were equally important in reconstituting it here, as were comments by Carla Cacciari and Flavio Fusi Pecci. I am grateful to them all. It is again a special pleasure to thank David Sandage for preparing the diagrams for press.

REFERENCES

Aaronson, M. 1986 in Star Forming Dwarf Galaxies and Related Objects, eds. D. Kunth, T.X. Thaun, & J.T.T Van (Paris: Ed Front.) p. 125

Alcock, C. et al. 1998, ApJ, 492, 190

Alcock, C. 2000, AJ, 119, 2194

Alves, D.R., Bond, H.E., & Onken, C. 2001, AJ, 121, 318

Arp, H.C. 1955, AJ, 60, 317

Arp, H.C., Baum, W.A., & Sandage, A. 1953, AJ, 58, 4

Bencivenni, D., Caputo, F., Manteign, M., & Quarta, M.L. 1991, ApJ, 380, 484

Bingham, E.A., Cacciari, C., Dickens, R.J., & Fusi Pecci, F. 1984, MNRAS, 209, 765

Blanco, V. 1992, AJ, 104, 734

Bono, G., Caputo, F., Cassisi, S., Castellani, V., & Marconi, M. 1997a, ApJ, 479, 279

Bono, G., Caputo, F., Cassisi, S., Incerpi, R., & Marconi, M. 1997b, ApJ, 483, 811

Bono, G., Caputo, F., & Stellingwerf, R.F. 1994, ApJ, 423, 294

Bono, G., Caputo, F., & Stellingwerf, R.F. 1995, ApJS, 99, 263

Borissova, J., Catelan, M., & Valchev, T. 2001, MNRAS, 324, 77

Brocato, E., Castellani, V., & Ripepi, V. 1994, AJ, 107, 622 (NGC 4590)

Brocato, E., Castellani, V., & Ripepi, V. 1996, AJ, 111, 890

Butler, D. 1975, ApJ, 200, 68

Butler, D., Dickens, R.J., & Epps, E. 1978, ApJ, 225, 148

Cacciari, C. 1979, AJ, 84, 1542

Cacciari, C. & Clementini, G. 2004, in Standard Candles for the Extragalactic Distance Scale, ed. D. Alloin, W. Gieren (Springer, Berlin), p. 105

Cacciari, C., Corwin, T.M., & Carney, B.W. 2004, astro/ph 0409567

Caldwell, N., Armandroff, T.E., DaCosta, G.S., & Seitzer, P. 1998, AJ, 115, 535

Caloi, V., D'Antona, F. & Mazzitelli, I, (1997), A&A, 320, 823

Caputo, F. 1988, A&A, 189, 70

Caputo, F. 1997, MNRAS, 284, 994

Caputo, F., Castellani, V., Marconi, M, & Ripepi, V 1999, MNRAS, 306, 815

Caputo, F., Castellani, V., Marconi, M., & Ripepi, V. 2000, MNRAS, 316, 819 (CCMR)

Caputo, F., DeRinaldis, A., Manteiga, M., Pulone, L., & Quarta, M.L. 1993, A&A, 276, 41

Carney, B.W., Storm, J., & Jones, R.V. 1992, ApJ, 386, 663 (CSJ)

Carney, B.W., Storm, J., Trammell, S.R., & Jones, R.V. 1992, PASP, 104, 44

Cassisi, S., Castellani, V., Degl'Innocenti, S., Salaris, M., & Weiss, A. 1999, A&AS, 134, 103

Castellani, V, Chieffi, S., & Pulone, L. 1991, ApJS, 76, 911

Castelli, F., 1999, A&A, 346, 564

Catalan, M. 2004, in Variable Stars in the Local Group, eds. D.W. Kurtz & K.R. Pollard; IAU Coll. 193. ASDP Conf Ser. 310, p 113

Catelan, M., Pritzl, B.J., & Smith, H.A. 2004, ApJS, 155, 633

Chiosi, C., Wood, P., Bertelli, G., & Bressan, A. 1992, ApJ, 387, 320

Cho, D-H., Lee, S-G., Jeon, Y-B., & Sim, K.J. 2005, AJ, 129, 1922

Clementini et al. 2004, in Variable Stars in the Local Group, eds. D.W. Kurtz & K.R. Pollard; IAU Col. 193. ASP Conf. Ser 310, p. 60

Clementini, G., Gratton, R., Bragaglia, A., Carretta, E., Di Fabrizio, L, & Maio, M. 2003, AJ, 125, 1309

Clement, C.M. 2001, The new cluster variable catalog accessed at http://www.astro.utoronto.ca/people.html

Clement, C.M., & Shelton, L. 1999a, AJ, 118, 453

Clement, C.M., & Sheldon, L. 1999b, ApJ, 515, L85

Clube, S.V.M., Evans, D.S.E., & Jones, D.H.P. 1969, Mem. RAS., 72, 101

Corwin, T.M., & Carney, B.W. 2001, AJ, 122, 3183

Corwin, T.M., Carney, B.W., & Nifong, B.G. 1999, AJ, 118, 2875

Cox, A.N. 1987, in Second Conference on Faint Blue Stars, IAU Colloquim No. 95, Ed. A.G.D. Philip, D.S. Hayes, & J.W. Leibert (Davis, Schenectady), p 161

Cox, A.N., Hodson, S.W., & Clancy, S.P. 1983, ApJ, 266, 94

Cox, A.N., King, D.S., & Hodson, S.W. 1980, ApJ, 236, 219

Cseresnjes, P. 2001, AA, 375, 909

Dall'Ora, M. et al. 2003, AJ, 126, 197

Demarque, P., Zinn, R., Lee, Y-W., & Yi, S. 2000, AJ, 1398

DeSantis, R., & Cassisi, S. 1999, MNRAS, 308, 97

Dickens, R.J. 1971, ApJS, 22, 249

Dickens, R.J., & Flinn, R. 1972, MNRAS, 158, 99

Dorman, B. 1992, ApJS, 81, 221

Eggen, O.J. 1977, ApJ, 215, 812

Eggen, O.J., Lynden-Bell, D., & Sandage, A. 1962, ApJ, 136, 748

Eggen, O.J., & Sandage, A.R. 1959, MNRAS, 119, 255

Epstein, I. 1969, AJ, 74, 1131

Fitch, W., Wisniewski, W., Johnson, H.L., 1966, Arizona Comm, 5, 71, parts 2, 3

Freeman, K.C. 1987, ARAA, 25, 603

Freeman, K.C., & Bland-Hawthorn, J. 2002, ARAA, 40, 487

Gratton, R.G. 1998, MNRAS, 296, 739

Gratton, R.G., Tornambe, A., & Ortononi, S. 1986, A&A, 169, 111

Gratton, R.G., Fusi Pecci, F., Carretta, E., Clementini, G., Corsi, C.E., & Lattanzi, M. 1997, ApJ, 491, 749

Grosse, E. 1932, Astron. Nach., 246, 376

Hachenberg, O. 1939, Zs.f.Ap, 18, 49

Harris, W.E. 1996, AJ, 112, 1487

Ibata, R., Gilmore, G., & Irwin, M.J. 1994, Nature, 370, 194

Ibata, R., Gilmore, G., & irwin, M.J. 1995, MNRAS, 277, 781

Ivezic, Z. et al. 2000, AJ, 120, 963

Kaluzny, J., Olech, A., & Stanek, K.Z. 2001, AJ, 121, 1533

Kholopov, P.N. 1985, General Catalog of Variable Stars, 4th ed. (Nauka, Moscow)

Kinman, T.D. 1961, Roy. Obs. Bull., E37

Kovacs, G., Buchler, J.R., Marom, A., Iglesias, C.A., & Rogers, F.J. 1992, A&A, 259, L46

Layden, A.C. 1994, AJ, 108, 1016

Layden, A.C. 1995, AJ, 110, 2312

Lee, Y.-W. 1990, ApJ, 363, 159

Lee, J-W., & Carney, B.W. 1999a, AJ, 117, 2868

Lee, J-W., & Carney, B.W. 1999b, AJ, 118, 1373

Lee, Y.-W., Demarque, P., & Zinn, R. 1990, ApJ, 350, 155 (LDZ)

Lub, J. 1979, AJ, 84, 383

Lynden-Bell, D., & Lynden-Bell, R.M. 1995, MNRAS, 275, 429

Mackey, A.D., & Gilmore, G.F. 2003, MNRAS, 345, 747

Majewski, S.R. 1993, ARAA, 31, 575

Mateo, M. 1996, in Formation of the Galctic Halo...Inside and Out; Conf. Ser. 92, eds. H. Morison, & A. Sarajedini, p. 434

Mateo, M. 1998, ARAA, 36, 435

McCarthy, P.J. 2004, ARAA, 42, 477

McNamara, D.H., Rose, M.B., Brown, P.J., Ketcheson, D.I., Maxwell, J.E., Smith, K.M., & Wooley, R.C. 2004, in Variable Stars in the Local Group, ASP Conf. Ser. 310, 525

Menzies, J. 1974, MNRAS, 168, 177

Montegriffio, P., Ferraro, F.R., Origlia, L., & Fusi Pecci, F. 1998, MNRAS, 297, 872

Nemec, J.M. 2004, AJ, 127, 2185

Newberg, H.J. et al. 2002, ApJ, 569, 245

Nikolov, N., Buchantsova, & Frolov, M. 1984, "The Mean Light and Color of 210 Field RR Lyrae Type Stars", Astron. Council USSR Acad. Sci. Sofia

O'Connell, D. 1958, ed. Stellar Populations, Specola Vaticana, RicA, 5

Olech, A., Kaluzny, J., Thompson, I.B., Pych, W., Krzeminski, W., & Schwarzenberg-Czerny, A. 1999, AJ, 118, 442

Olech, A., Kaluzny, J., Thompson, I.B., Pych, W., Krzeminski, W., & Schwarzenberg-Czerny, A. 2001, MNRAS, 321, 421

Oosterhoff, P. Th. 1939, Observatory, 62, 104

Oosterhoff, P. Th. 1944, BAN, 10, 55

Paczynski, B. 1965a, Acta Astron. 15, 103

Paczynski, B. 1965b, Acta Astron. 15, 115

Paczynski, B. 1966, Acta Astron. 16, 97

Peterson, J.O. 1973, A&A, 27, 89

Peterson, J.O. 1978, A&A, 62, 205

Peterson, J.O. 1979, A&A, 80, 53

Piersimoni, A.M., Bono, G., & Ripepi, V. 2002, AJ, 124, 1528

Preston, G.W. 1959, ApJ., 130, 507

Preston, G.W. 1961, ApJ, 133, 29

Preston, G.W., & Paczynski, B., 1964, ApJ, 140, 181

Pritzl, B.J., Smith, H.A., Catelan, M., & Sweigart, A.V. 2001, AJ, 122, 2600

Pritzl, B.J., Armandroff, T.E., Jacoby, G., and DaCosta, G.S. 2002, AJ, 124, 949

Pritzl, B, Smith, H.A., Catelan, M., & Sweigart, A.V. 2000, ApJ, 530, L41

Pritzl, B., Smith, H.A., Catelan, M., & Sweigart, A.V. 2001, AJ, 122, 2600

Rich, R.M. et al. 1997, ApJ, 484, L25

Salaris, M, Degl'Innocenti, S., & Weiss, A. 1997, ApJ, 479, 665

Sandage, A. 1953, AJ, 58, 61

Sandage, A. 1958, in Stellar Populations, Specola Vaticana, ed. D. O'Connell, RicA, 5, 41

Sandage, A. 1969, ApJ, 157, 515

Sandage, A. 1981a, ApJ, 244, L23 (S81a)

Sandage, A. 1981b, ApJ, 248, 161 (S81b)

Sandage, A. 1982a, ApJ, 252, 553 (S82a)

Sandage, A. 1982b, ApJ, 252, 574 (S82b)

Sandage, A. 1990a, ApJ, 350, 603 (S90a)

Sandage, A. 1990b, ApJ, 350, 631 (S90b)

Sandage, A. 1990c, JRASC, 84, 70

Sandage, A. 1993a, AJ, 106, 687 (S93a)

Sandage, A. 1993b, AJ, 106, 703 (S93b)

Sandage, A. 2004, AJ, 128, 858

Sandage, A., Bell, R.A., & Trippico, M.J. 1999, ApJ, 522, 250

Sandage, A., & Cacciari, C. 1990, ApJ, 350, 645

Sandage, A., Katem, B.N., & Sandage, M. 1981, ApJS, 46, 41 (SKS)

Sandage, A., Smith, L.L., & Norton, R.H. 1966, ApJ, 44, 894

Sandage, A., & Wildey, R., 1967, ApJ, 150, 469

Sawyer Hogg, H. 1973, Third Catalogue of Variable Stars in Globular Clusters, David Dunlap Obs. Pub 3, No. 6

Schwarzschild, M. 1958, in Stellar Populations, Specola Vaticana, ed. D. O'Connell, RicA, 5, 59

Searle, L., & Zinn, R. 1978, ApJ, 225, 357

Sekiguchi, M, & Fukugita, M. 2000, AJ, 120, 1072

Siegel, H.M. & Majewski, S.R. 2000, AJ, 120, 284

Simon, N.R., & Clement, C.M. 1993, ApJ, 410, 526

Skillman, E.D., Kennicutt, R.C., & Hodge, P. W. 1989, ApJ, 347, 875

Stepien, K. 1972, Acta Astron. 22, 175

Storm, J., Carney, B.W., & Beck, J.A. 1991, PASP, 103, 1264

Sturch, C.R. 1966, ApJ, 143, 774

Sturch, C.R. 1977, PASP, 89, 349

Suntzeff, N.B., Kinman, T.D., & Kraft, R.P. 1991, ApJ, 367, 528

Sweigart, A.V., & Gross, P.G. 1976, ApJS, 32, 367

Sweigart, A.V., Renzini, A., & Tonambe, A. 1987, ApJ, 312, 762

Tammann, G.A., Sandage, A. & Reindl, B. 2003, A&A, 404, 423

van Albada T.S., & Baker, N. 1973, ApJ, 1185, 477

van den Bergh, S. 1967, AJ, 72, 70

van den Bergh, S., & Mackey, A.D., 2004, MNRAS, 354, 713

VandenBerg, D.A., Swenson, F.J., Rogers, F.J., Iglesias, C.A., & Alexander, D.R. 2000, ApJ, 532, 430

Vivas, A.K., & Zinn, R. 2002, Astro/ph 02121116

Vivas, A.K., & Zinn, R. 2004, MSAIt, 74, 928

Vivas, A.K. et al. 2001, ApJ, 554, L33

Walker, A.R. 1994, AJ, 108, 555

Walker, A.R. 1998, AJ, 116, 220

Walker, A.R., & Nemec, J.M. 1996, AJ, 112, 2026

Wehlau, A., Slawson, R.W., & Nemec, J.M. 1999, AJ, 117, 286

Yanny, B., et al. 2000, AJ, 120, 963

Zinn, R., & West, M.J. 1984, ApJS, 55, 45

This preprint was prepared with the AAS LaTeX macros v5.2.

Figure Captions

Figure 1. Distribution of period with metallicity for the 302 type ab (fundamental mode) RR Lyrae variables studied by Layden (1994, 1995). The full line [Eq. (1) of the text] is an approximation to the envelope of the shortest period variables at a given metallicity. The dashed line is Eq. (2) of the text for the log P values averaged over the narrow intervals of [Fe/H] listed in Table 1.

Figure 2. The data from Fig. 1 for the Layden field star sample but with three linear envelope lines of Eqs. (3), (4) and (4') superposed. The envelope line is the same as in Fig. (1) for [Fe/H] more metal rich than -1.8 but two steeper envelopes from Eqs. (4) and (4') are shown as dashed lines for more metal poor stars.

Figure 3. The same data for field stars as in Fig. 1 but with the parabolic fit of an envelope line from Eq. (5) superposed.

Figure 4. The period-metallicity relation for 919 RR Lyrae stars in globular clusters from data in the Clement (2001) update of the Sawyer Hogg (1973) cluster variable catalog. Each cluster is represented by the horizontal line at its adopted metallicity from Harris (1996) on the metallicity scale of Zinn and West. The parabolic short-period locus for the field stars from Eq. (5) is shown. It fails to represent the short period distribution, requiring a shift of $\Delta \log P = 0.029 \pm .007$ toward longer periods for the cluster variables relative to those in the field.

Figure 5. The predicted run of log T_e with [Fe/H] keeping the luminosity fixed at the Catelan et al. (2004) calibration of Eq. (10), and using the four loci for the FBE period-metallicity envelopes from Eqs. (1), (3), (4), (4') and (5), together with the Bono et al. mass equation from Eq. (15). These have been put into the pulsation Eq. (16) to generate the curves. Line number 1 is for the linear envelope to the log P([Fe/H]) relation at the shortest periods in Fig. 1 (eq. 1); numbers 2 and 4 use the dashed lines in Fig. 2 from Eqs. (4) and (4') for [Fe/H] less than -1.8; number 3 is for the parabolic envelope of Eq. (5) from Fig. 3; number 5 is for the midpoint log P([Fe/H]) relation of Eq. (2) which is the dashed line in Fig. 1.

Figure 6. Five predicted runs of log T_e with [Fe/H] at the fundamental blue edge of the instability strip using a fixed parabolic envelope locus to the log P-[Fe/H] relation from Eq. (5) and Fig. 3, and five different RRL luminosity calibrations. Line 1 is for the linear luminosity calibration of Eq. (6) which was the S93a pulsation solution; line 2 is for the linear calibration of Clementini et al. (2003) from Eq. (12); line 3 is for the non-linear calibration of Eq. (7) by Caputo et al. (2000); line 4 is the non-linear calibration of Eq. (10) by Catelan et al. (2004); line 5 is for the two-line calibration of McNamana et al. (2004) of

Eqs. (13) and (14).

Figure 7. Predicted variation of B-V colors for the temperature curves in Fig. 5, using the Catelan et al. (2004) luminosity calibration in Eq. (10) and various assumed period-metallicity envelopes from Figs. 1-3. The conversion from the predicted temperatures in Fig. 5 to B-V is made using the adopted temperature-color relation of Eq. (18). Line 1 uses the linear envelope of equation 1, Fig. 1; lines 2 and 4 for [Fe/H] $<$ -1.8 are for the dashed lines in Fig 2 which are Eqs. (4) and (4'); line 3 is for the parabolic envelope of Fig. 3, Eq. (5), and line 5 is for the midpoint relation of Eq. (2).

Figure 8. Predicted variation of B-V colors for the temperature curves in Fig. 6 using the fixed period-metallicity envelope of Eq. (5), (Fig. 3), and the five different luminosity calibrations of Eqs. (6), (8), (10), (12), (13), and (14). The adopted temperature-color relation is Eq. (18). The identification of the lines is the same as in the caption to Fig. 6.

Figure 9. The points are the de-reddened photoelectric mean $(\text{B-V})^0_{\text{mag}}$ colors for 160 field RR Lyrae stars, plotted vs. Layden's measured [Fe/H] values, on the scale of Zinn and West. The line is the predicted run of color with metallicity from Eq. (19) calculated using the Catelan et al. (2004) luminosity calibration in Eq. (10) and the parabolic blue envelope locus to the period-metallicity relation of Fig 3, Eq. (5). The line is copied from Figs. 7 and 8.

Figure 10. The de-reddened colors of RRab stars in globular clusters for which the number of RRab variables is 10 or greater. The Oosterhoff period gap is more prominent than in Fig. 4 because of this restriction on the number of variables. The metallicity scale is that of Zinn and West, as listed by Harris (1996). The E(B-V) reddening values of individual clusters are also from Harris. The colors, not listed here, are on the system of $(\text{B-V})_{\text{mag}}$, transformed to that system by Table 4 of Bono et al. (1995) if a different mean color definition was used in the original literature. The line is the prediction of Eq. (19), calculated using the luminosity calibration of Catelan et al. [eq. (10)], and the parabolic period-metallicity envelope of Eq. (5), together with the color transformation of Eq. (18).

Figure 11. Combined data from Fig. 9 from field variables and from Fig. 10 for cluster variables. Crosses are the field stars. Dots are the cluster stars. The curve is from Eq. (20). It is similar to Eq. 19 for (Fe/H]) $>$ -2.0 but bends more strongly toward the red for more metal poor stars.

Table 1. THE MID-POINT RIDGE LINE OF THE PERIOD-METALLICITY CORRELATION IN FIGURE 1

Item (1)	⟨[Fe/H]⟩ (2)	Range of [Fe/H] (3)	n (4)	⟨log P⟩ (5)	$(B\text{-}V)^0_{mag}$ (6)
mean	-0.359	+0.07 to -0.70	21	-0.378	0.340
rms	0.049			0.015	0.011
mean	-0.983	-0.71 to -1.19	16	-0.329	0.335
rms	0.039			0.011	0.013
mean	-1.468	-1.20 to -1.79	71	-0.268	0.327
rms	0.019			0.007	0.005
mean	-1.991	-1.80 to -2.49	34	-0.217	0.329
rms	0.031			0.012	0.007
mean	-2.278	-2.06 to -2.49	7	-0.200	0.331
rms	0.059			0.018	0.025

Table 2. CLUSTERS WHOSE RR LYRAE COLOR DATA ARE USED IN FIGS. 10 & 11

Cluster	[Fe/H]	E(B-V)	n_{ab}	Literature
NGC 6362	-0.95	0.09	18	Olech et al. (2001)
NGC 6712	-1.01	0.45	7	Sandage et al.(1966)
NGC 6171	-1.04	0.33	15	Dickens (1971), Sandage (S90a)
NGC 6723	-1.12	0.05	23	Menzies (1974), (S90a)
NGC 6121	-1.20	var	31	Sturch (1977), Cacciari (1979)
NGC 1851	-1.22	0.02	21	Walker (1998)
NGC 5904	-1.27	0.03	91	Broccato et al. (1996), Storm et al. (1991), Caputo et al. (1999)
NGC 6981	-1.40	0.05	24	Dickens & Flinn (1972), (S90a)
NGC 6229	-1.43	0.01	30	Borissova et al. (2001)
NGC 6934	-1.54	0.10	68	Kaluzny et al. (2001)
NGC 5272	-1.57	0.01	145	Corwin & Carney (2001)
NGC 3201	-1.58	0.23	72	Piersimoni et al. (2002)
IC 4499	-1.60	0.23	63	Walker & Nemec (1996)
NGC 7089	-1.62	0.06	17	Lee & Carney (1999a)
NGC 7006	-1.63	0.05	53	Wehlau et al. (1999)
NGC 6809	-1.81	0.08	4	Olech et al. (1999)
NGC 4590	-2.06	0.07	13	Walker (1994)
NGC 5466	-2.22	0.00	13	Corwin et al. (1999)
NGC 7078	-2.26	0.10	39	Bingham et al. (1984)
NGC 5053	-2.29	0.04	5	Nemec (2004)
NGC 6341	2.28	0.02	11	Carney et al. (1992)

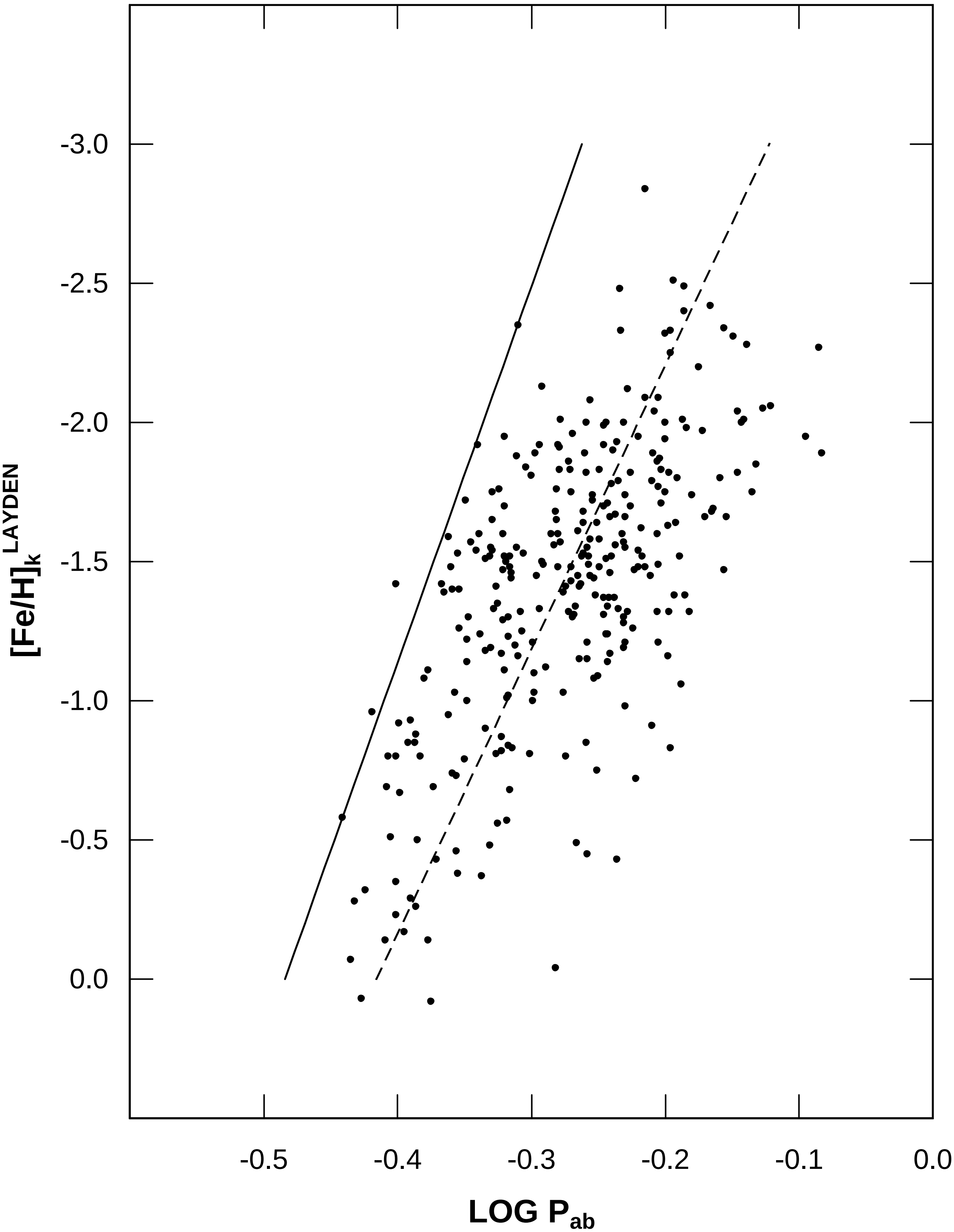

-3.0
-2.5
-2.0
-1.5
-1.0
-0.5
0.0
[Fe/H]k LAYDEN
-0.5
-0.4
-0.3
-0.2
-0.1
0.0
LOG Pab

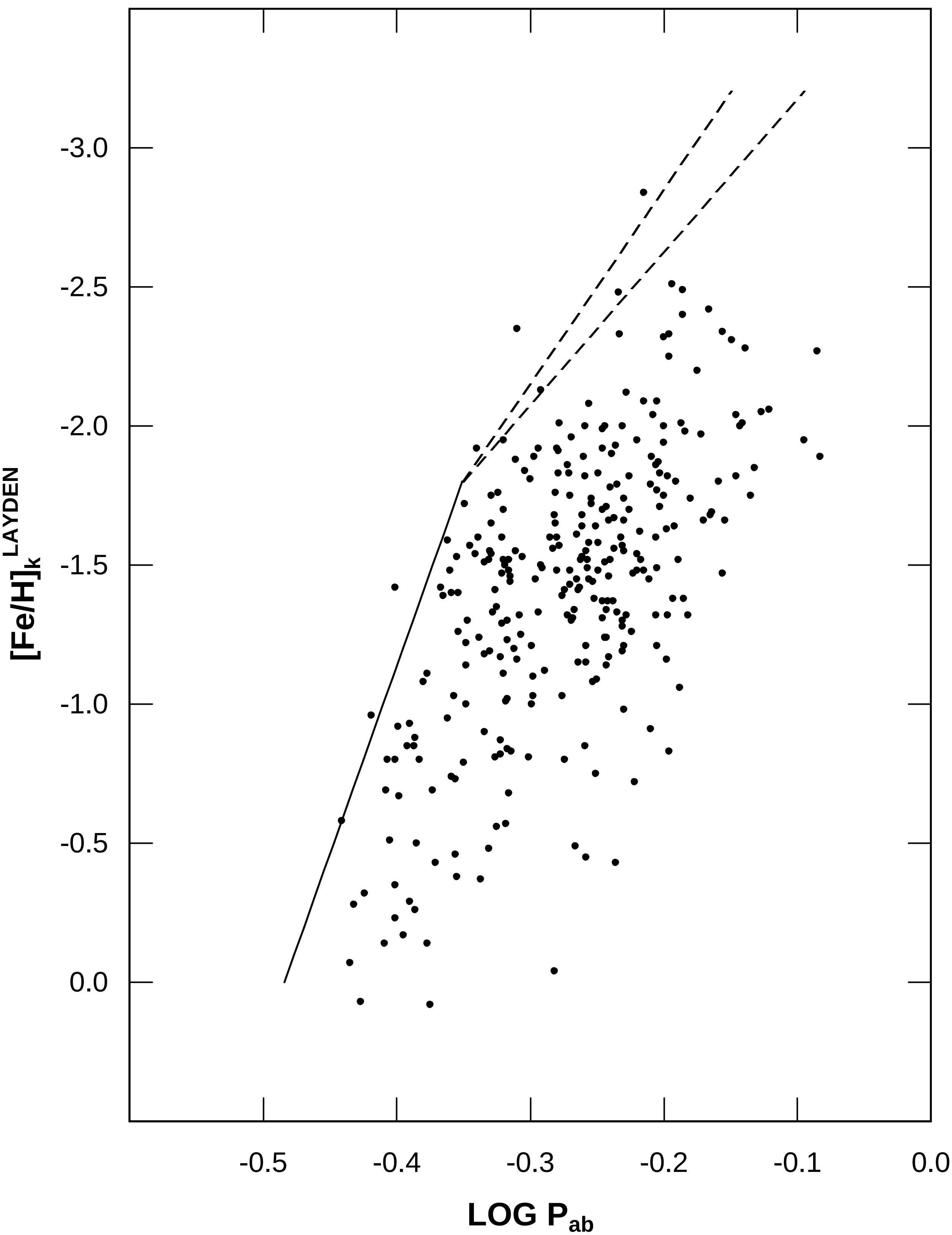

-3.0
-2.5
-2.0
-1.5
-1.0
-0.5
0.0
-0.5
-0.4
-0.3
-0.2
-0.1
0.0
[Fe/H]k LAYDEN
LOG Pab

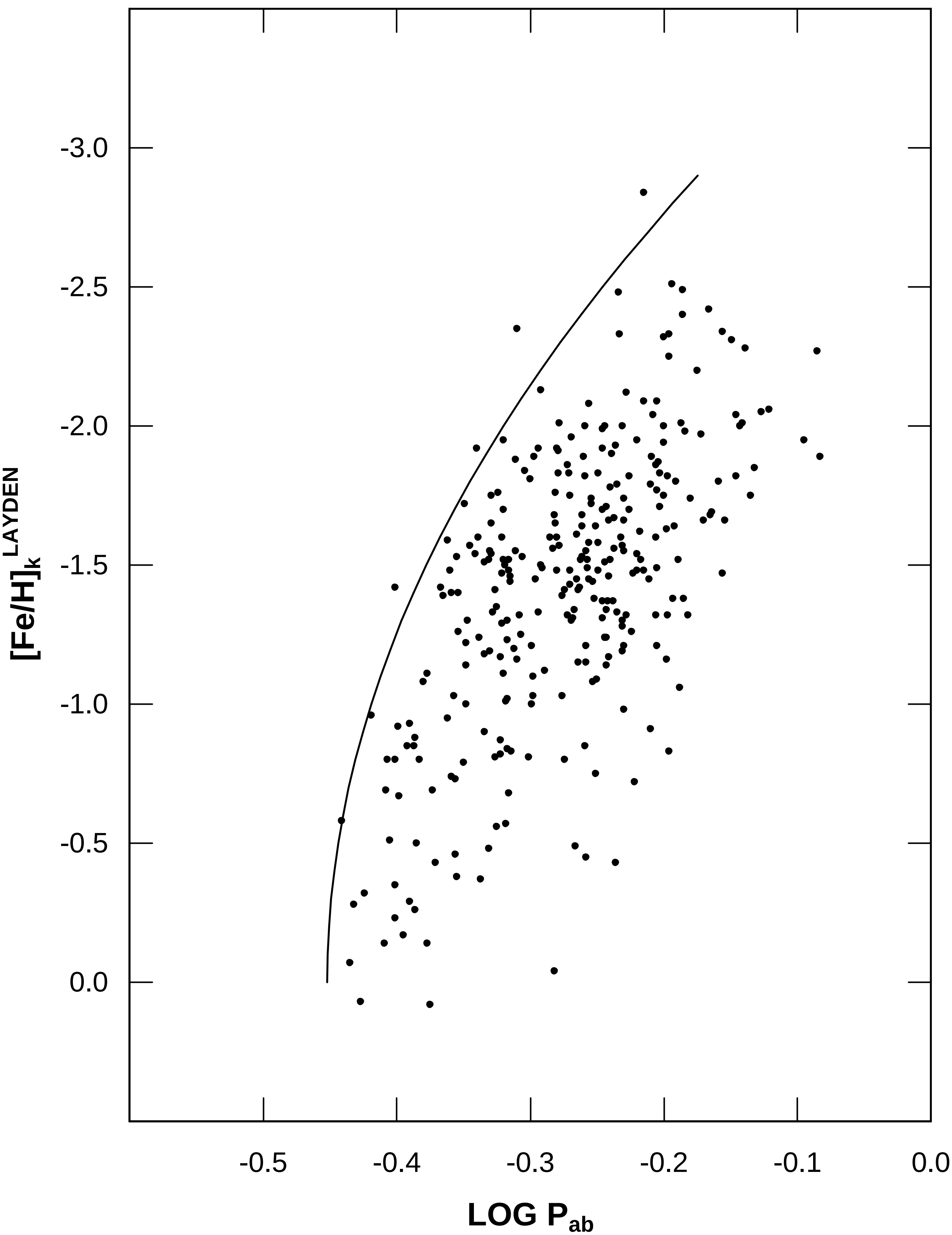

-3.0
-2.5
-2.0
-1.5
-1.0
-0.5
0.0
[Fe/H]k LAYDEN
-0.5
-0.4
-0.3
-0.2
-0.1
0.0
LOG Pab

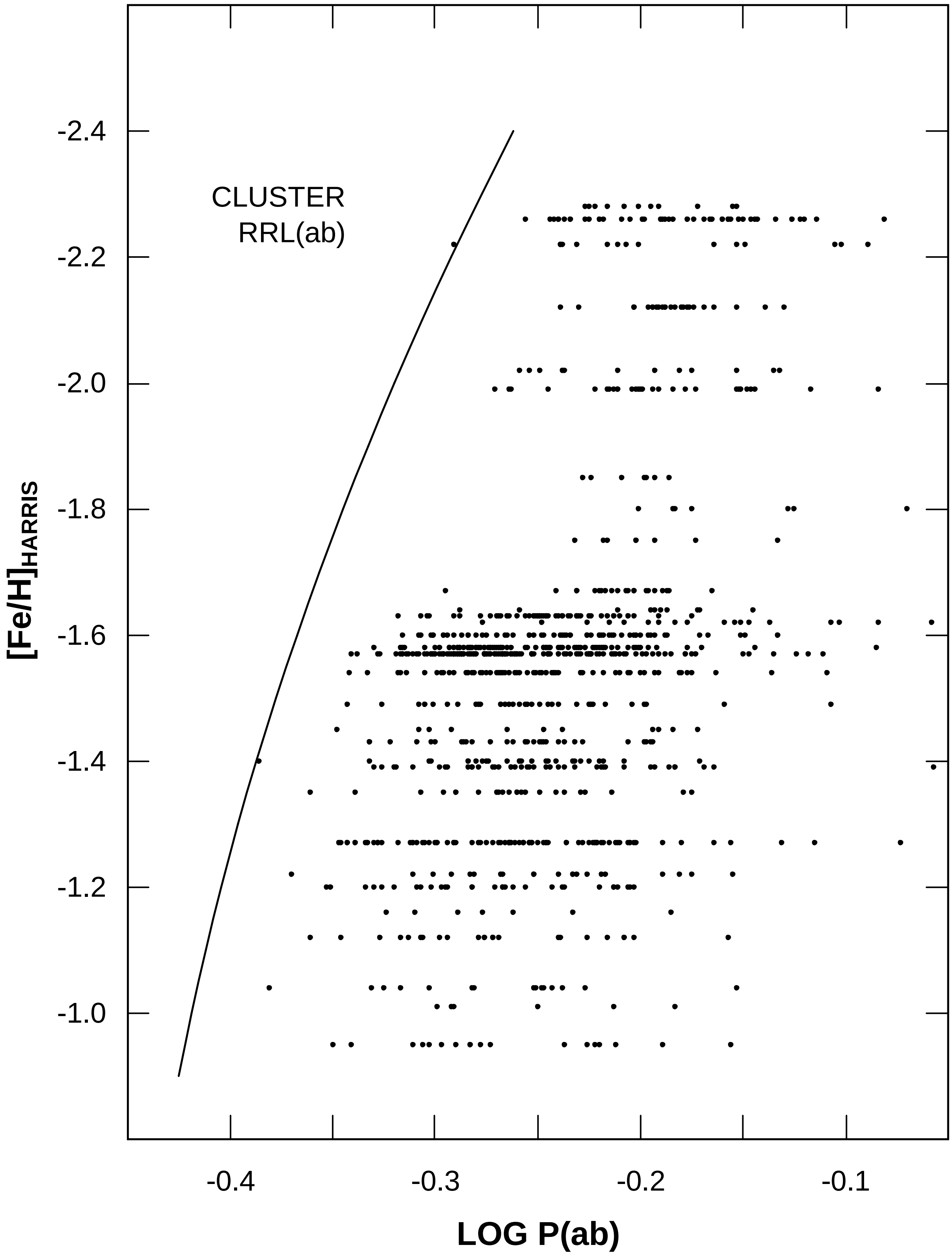
CLUSTER
RRL(ab)
-2.4
-2.2
-2.0
-1.8
-1.6
-1.4
-1.2
-1.0
[Fe/H]HARRIS
-0.4
-0.3
-0.2
-0.1
LOG P(ab)

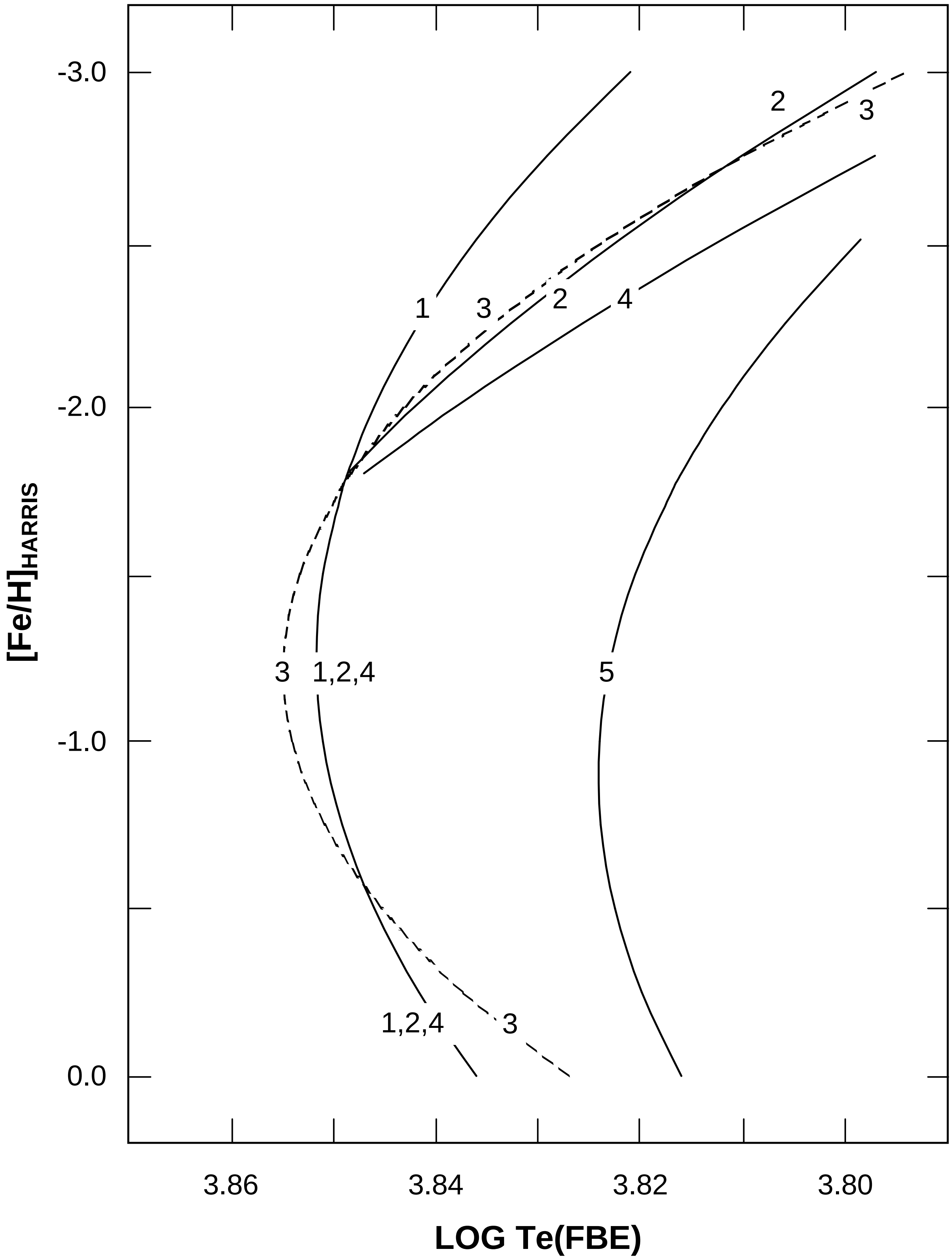

-3.0
-2.0
-1.0
0.0
3.86
3.84
3.82
3.80
[Fe/H]HARRIS
LOG Te(FBE)
1
2
3
4
5
1,2,4

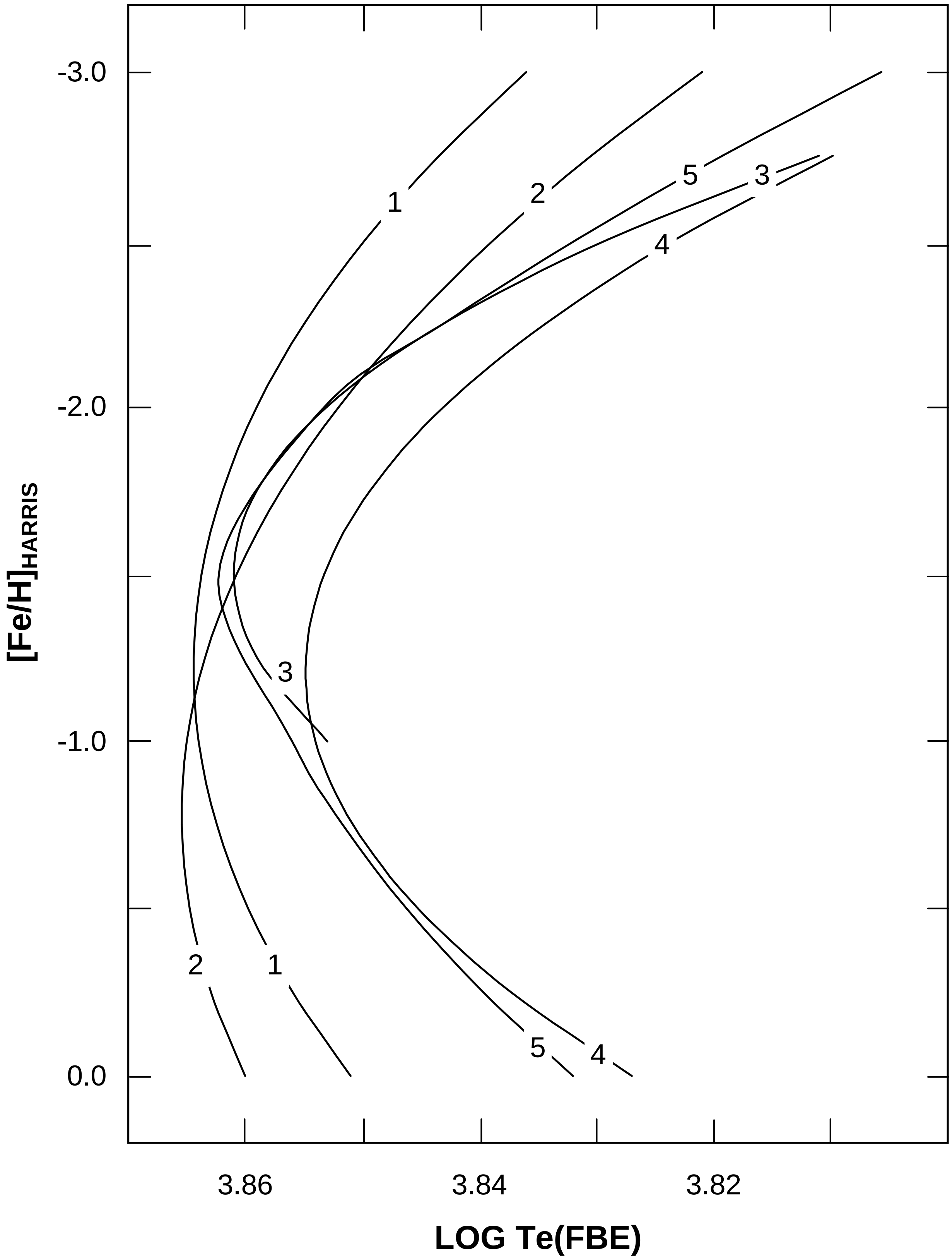
-3.0
-2.0
-1.0
0.0
[Fe/H]HARRIS
3.86
3.84
3.82
LOG Te(FBE)
1
2
5
3
4
3
2
1
5
4

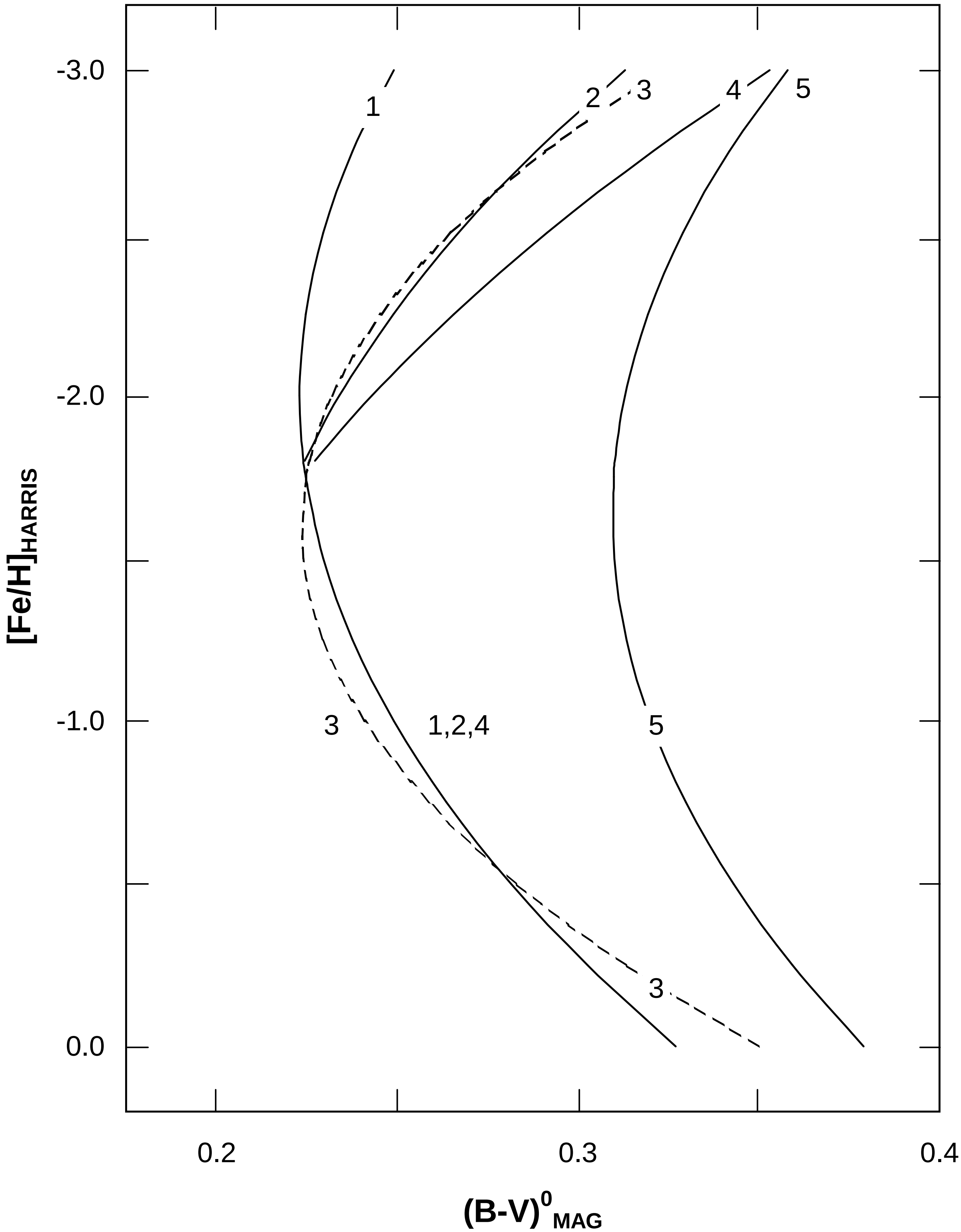

-3.0
-2.0
-1.0
0.0
0.2
0.3
0.4
[Fe/H]HARRIS
(B-V)0MAG
1
2
3
4
5
3
1,2,4
5
3

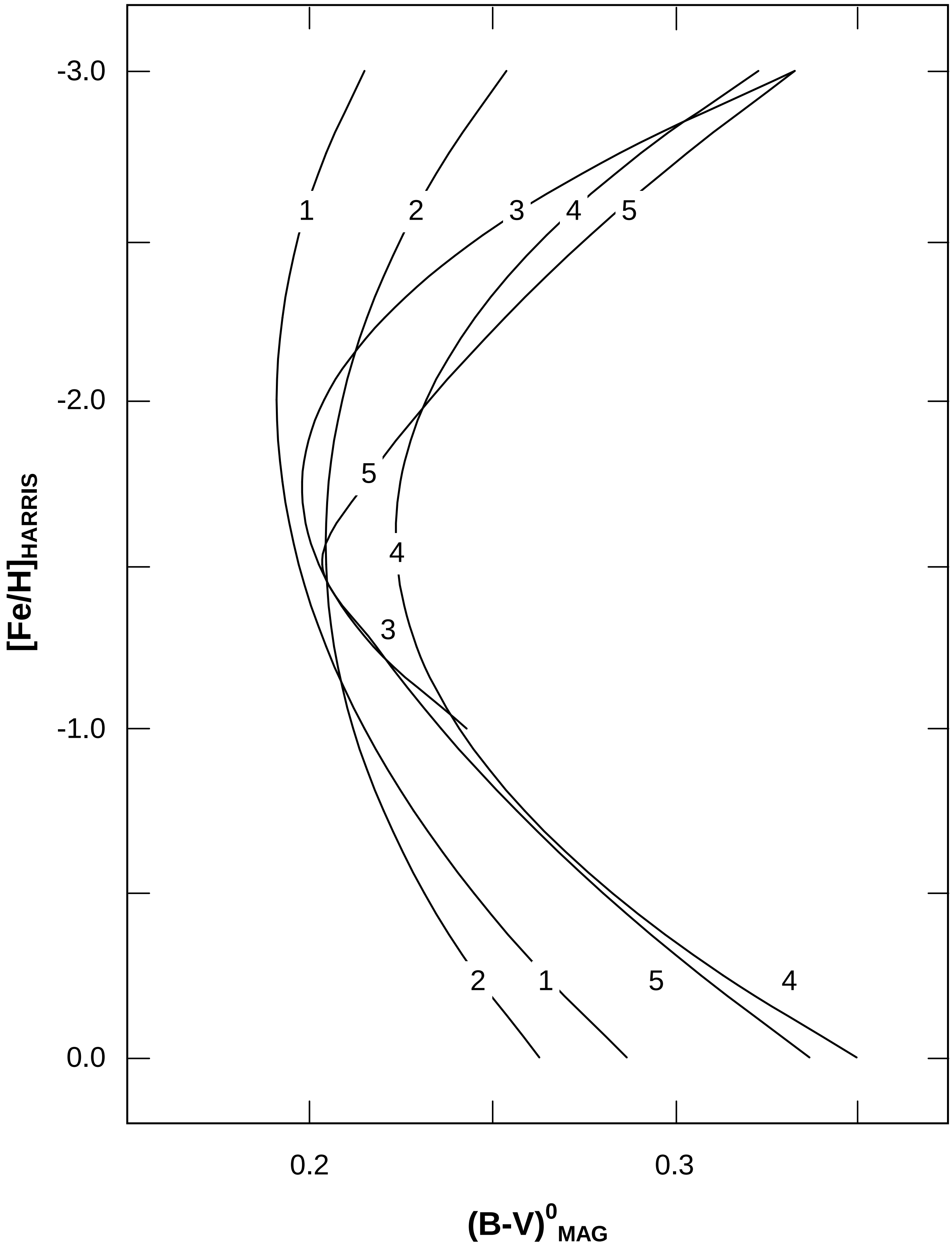

-3.0
-2.0
-1.0
0.0
[Fe/H]HARRIS
1
2
3
4
5
5
4
3
2
1
5
4
0.2
0.3
(B-V)0MAG

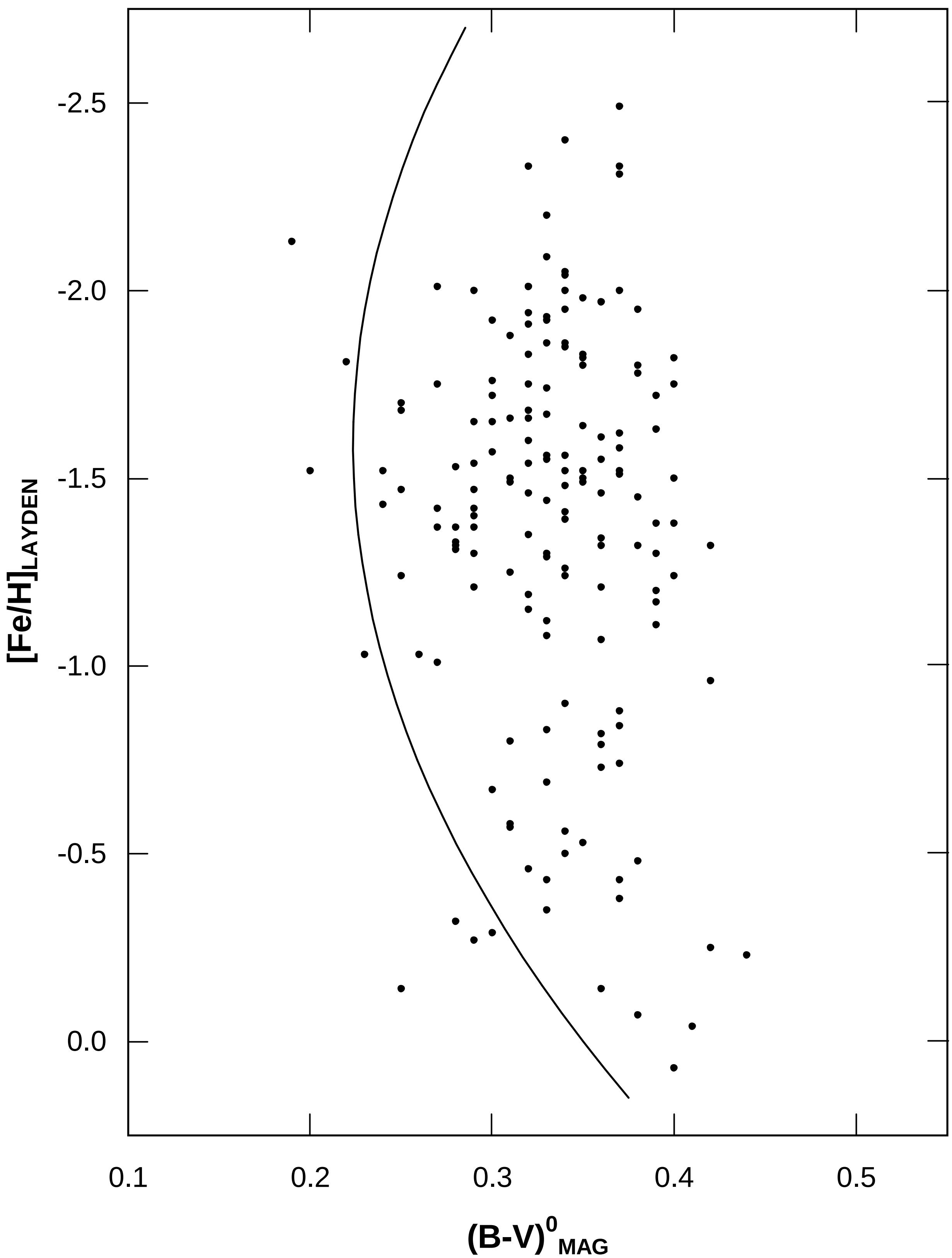

-2.5
-2.0
-1.5
-1.0
-0.5
0.0
[Fe/H]LAYDEN
0.1
0.2
0.3
0.4
0.5
(B-V)0MAG

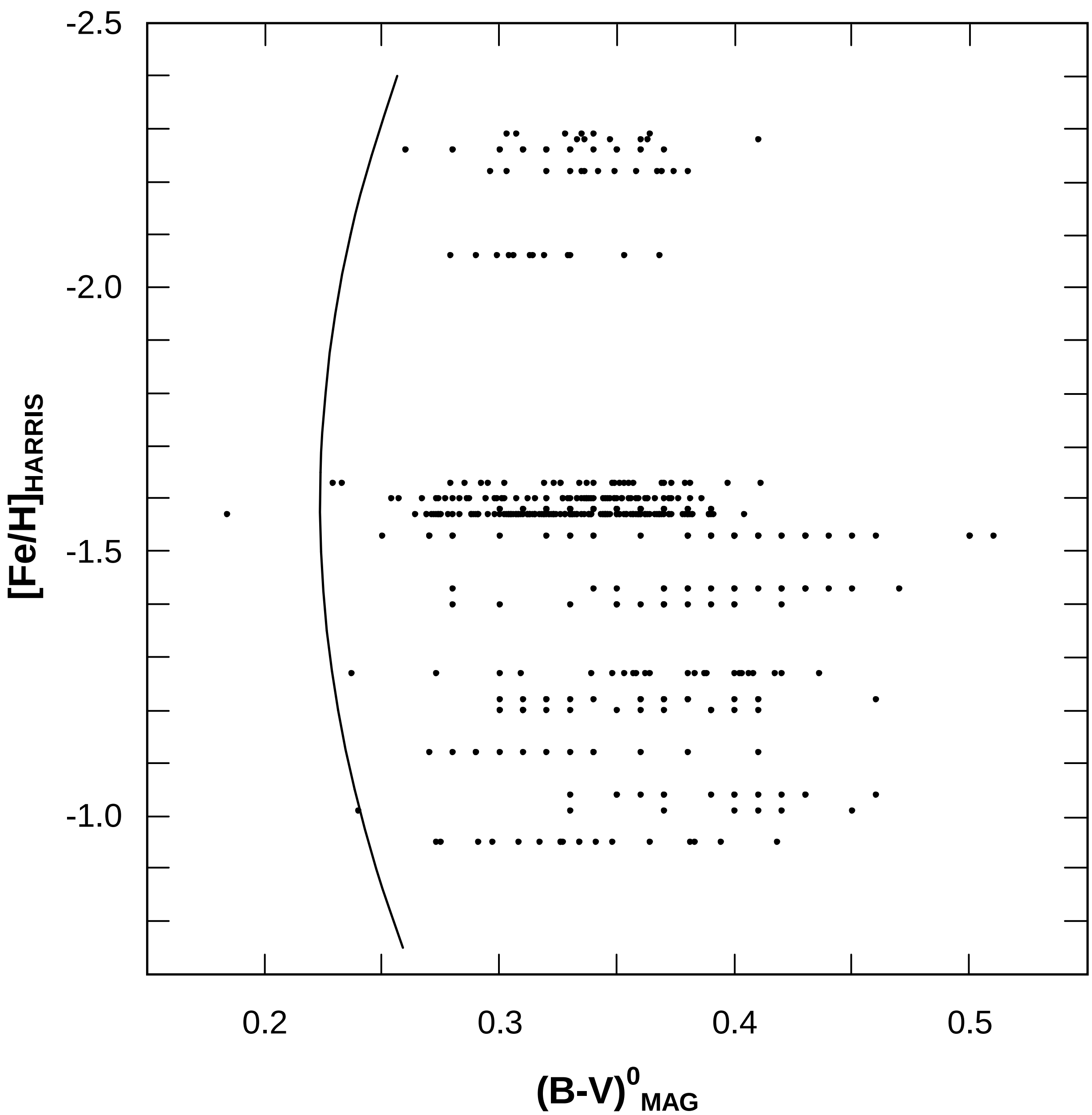
-2.5
-2.0
-1.5
-1.0
0.2
0.3
0.4
0.5
$[Fe/H]_{HARRIS}$
$(B-V)^0_{MAG}$

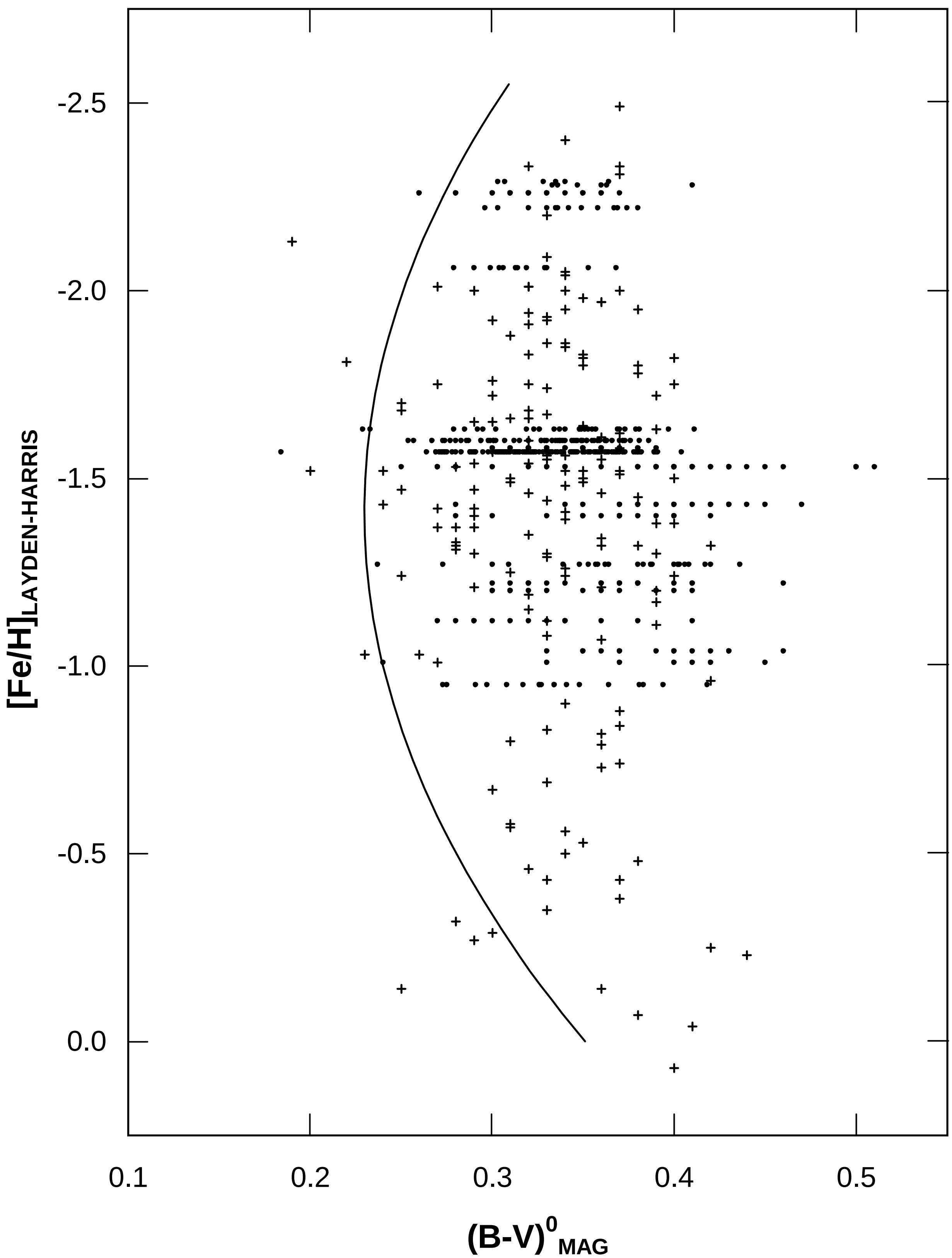

-2.5
-2.0
-1.5
-1.0
-0.5
0.0
0.1
0.2
0.3
0.4
0.5
[Fe/H]LAYDEN-HARRIS
(B-V)0MAG